(12) UK Patent (19) GB (11) 2609417 (13) B

(45) Date of B Publication 01.01.2025

(54) Title of the Invention: Ultrasonic transducer

(51) INT CL: ***A61B 17/32*** (2006.01) ***B06B 1/06*** (2006.01)

(21) Application No: **2110897.2**

(22) Date of Filing: **29.07.2021**

(43) Date of A Publication **08.02.2023**

(56) Documents Cited:

EP 1849444 A1 **WO 2018/134556 A1**

CN 104161619 A

Iula et al., "P2I-4 Design and Experimental Characterization of an Composite Longitudinal-Flexural Mode Ultrasonic Transducer", 2007 IEEE Ultrasonics Symposium Proceedings, pages 1693-1696. Published [online] 26 Dec 2007 by IEEE. Accessed 18 Nov 2021.

Fenu et al., "Progress Towards the Miniaturization of an Ultrasonic Scalpel for Robotic Endoscopic Surgery Using Mn:PIN-PMN-PT High Performance Piezocrystals", 2020 IEEE International Ultrasonics Symposium (IUS), pages 1-4. Published [online] 17 Nov 2020 by IEEE. Accessed 18 Nov 2021.

Li et al., "An Enhanced Hemostatic Ultrasonic Scalpel Based on the Longitudinal-Torsional Vibration Mode", IEEE Access, vol. 9, pages 10951-10961. Published 8 Jan 2021 by IEEE. Accessed 18 Nov 2021.

(58) Field of Search:

As for published application 2609417 A viz:

INT CL **A61B, A61F, B06B**

Other: **WPI, EPODOC, Patent Fulltext, INSPEC, BIOSIS, MEDLINE, XPESP, XSPRNG, XPI3E**

updated as appropriate

Additional Fields

INT CL **H02N**

Other: **None**

(72) Inventor(s):

Nicola Giuseppe Fenu
Sandy Cochran
Margaret Lucas
Rupert Shingleton
Rebecca Shirley Cleary

(73) Proprietor(s):

Nami Surgical Limited
Wilson Business Park, 1 Queen Elizabeth Avenue, Hillington Park, Glasgow, Renfrewshire, G52 4NQ, United Kingdom

(74) Agent and/or Address for Service:

Lincoln IP
4 Rubislaw Place, Aberdeen, AB10 1XN, United Kingdom

GB 2609417 B

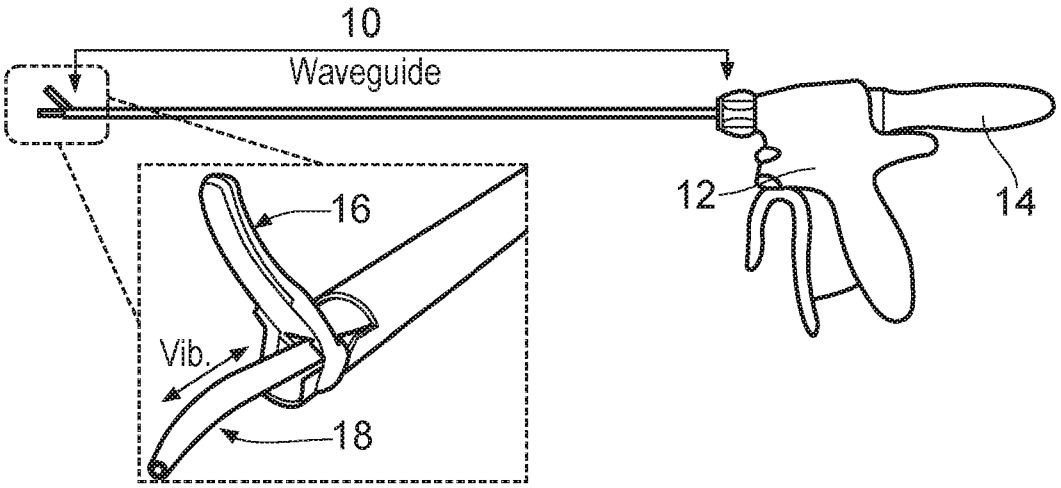


FIG. 1

28 10 22

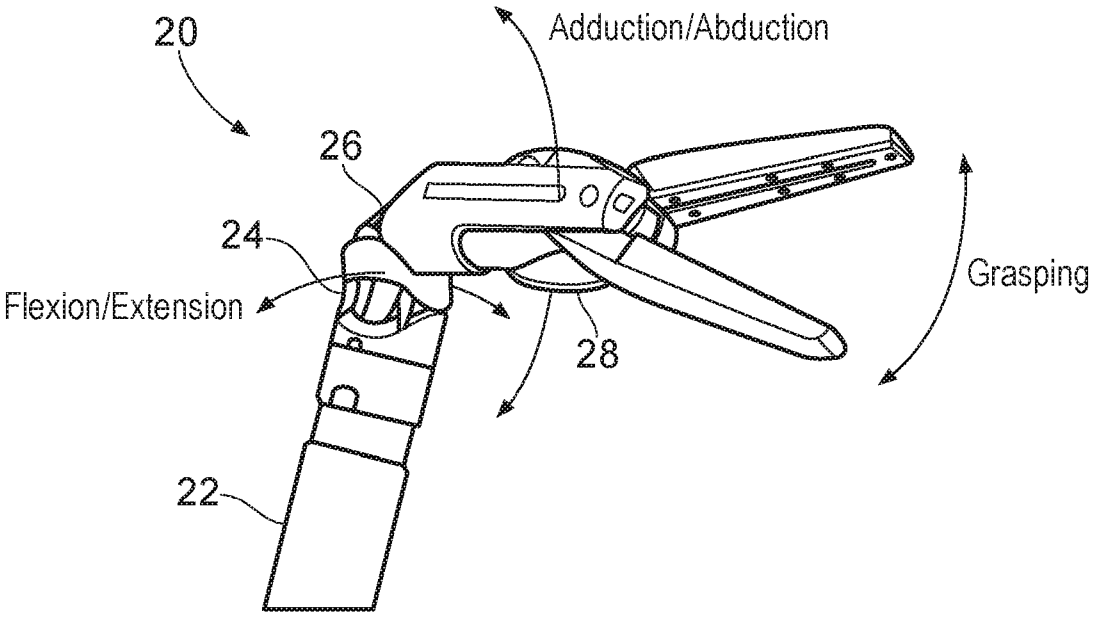


FIG. 2

28 10 22

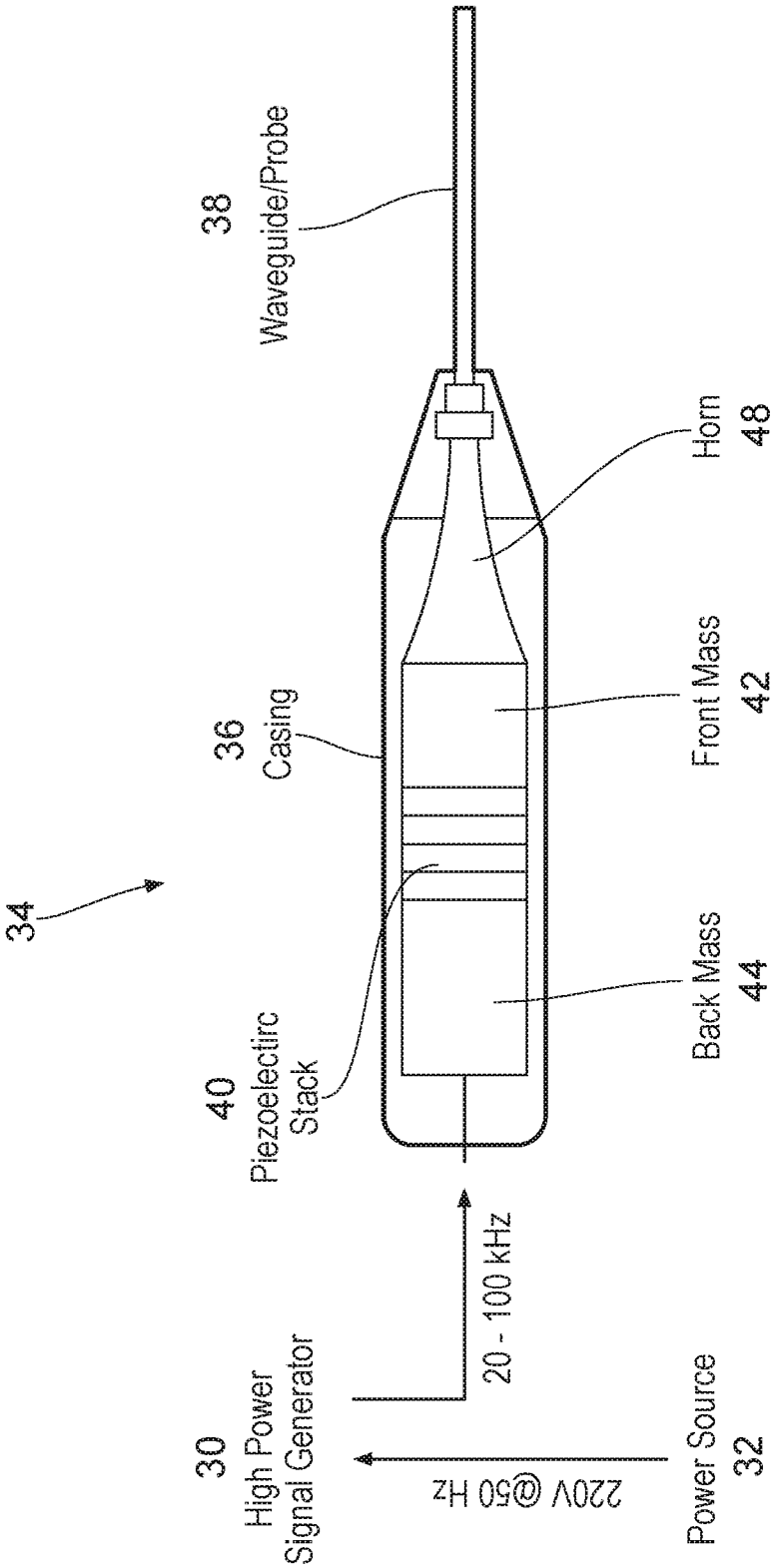

34
38
Waveguide/Probe
36
Casing
40
Piezoelectirc
Stack
Horn
48
Front Mass
42
Back Mass
44
30
High Power
Signal Generator
20 - 100 kHz
220V @50 Hz
Power Source
32

FIG. 3

28 10 22

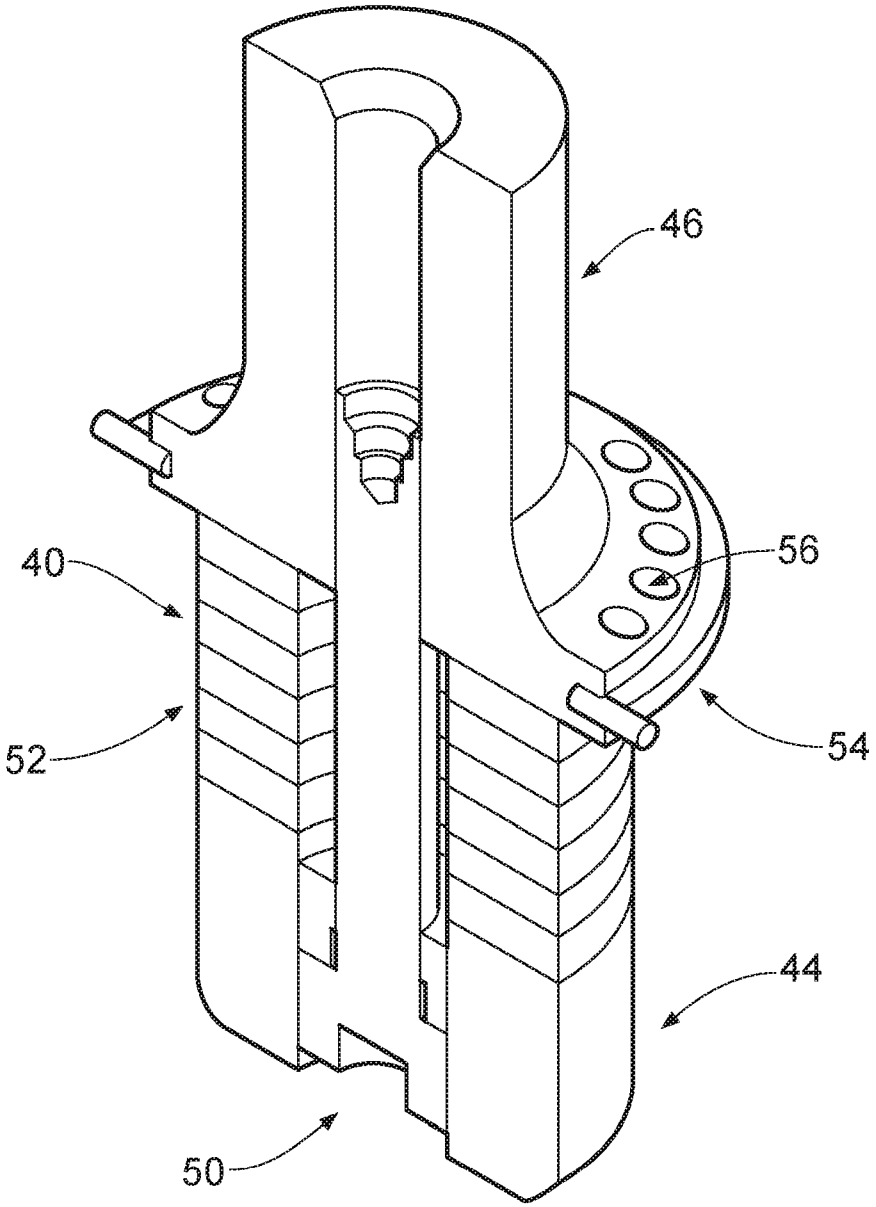


FIG. 4

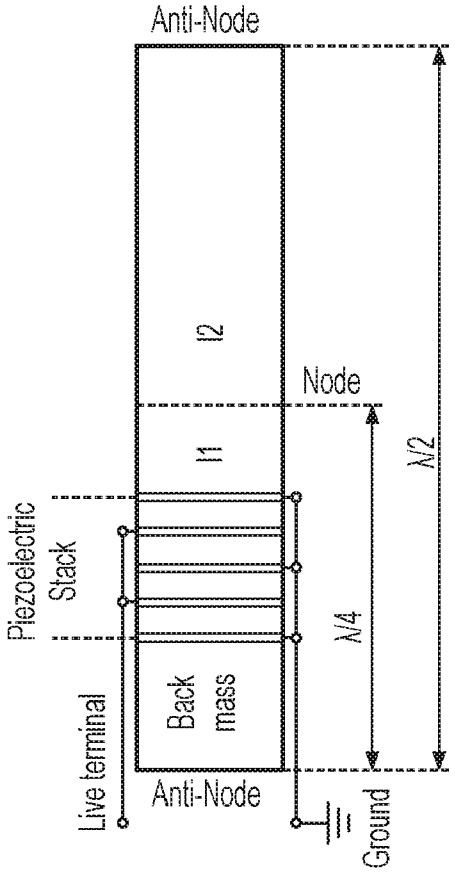

Anti-Node
l2
Node
l1
λ/2
λ/4
Piezoelectric
Stack
Back
mass
Live terminal
Anti-Node
Ground

FIG. 5B

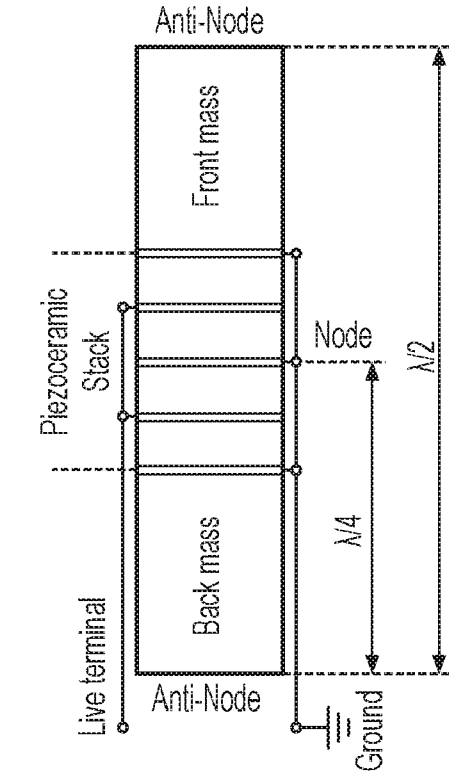

Anti-Node
Front mass
Node
λ/2
λ/4
Piezoceramic
Stack
Back mass
Live terminal
Anti-Node
Ground

FIG. 5A

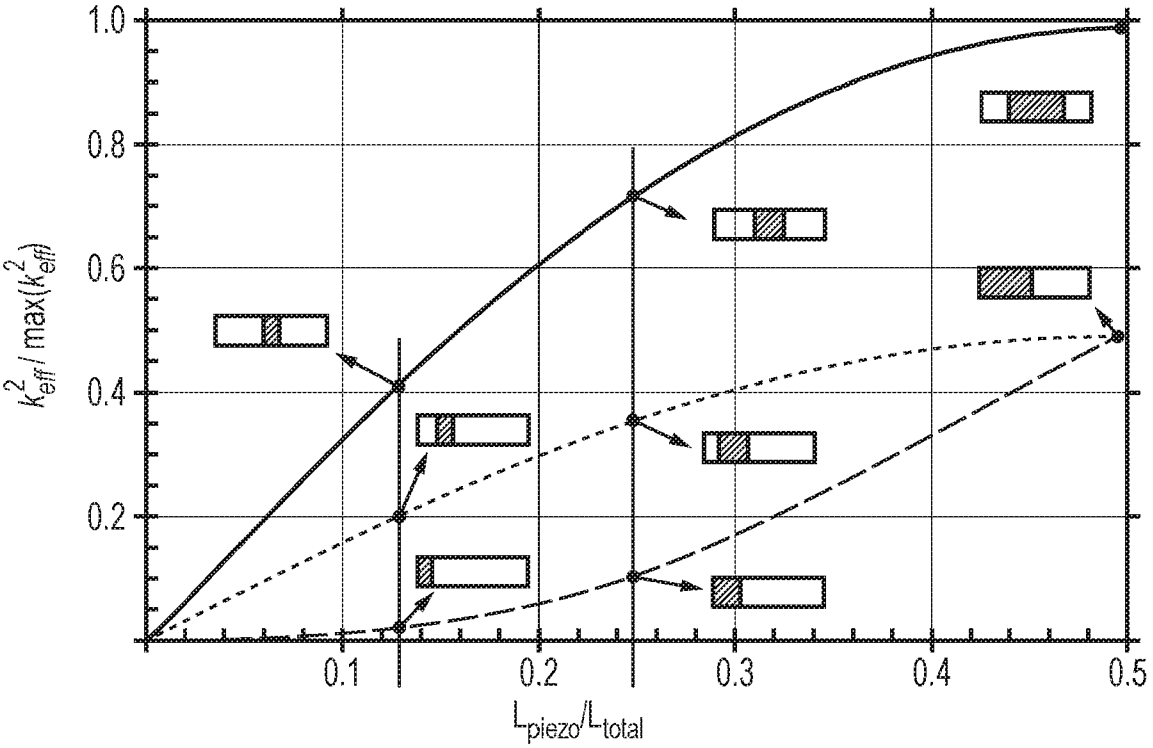

1.0
0.8
0.6
0.4
0.2
0.1
0.2
0.3
0.4
0.5
$k_{eff}^2 / \max(k_{eff}^2)$
L_{piezo}/L_{total}

FIG. 6A

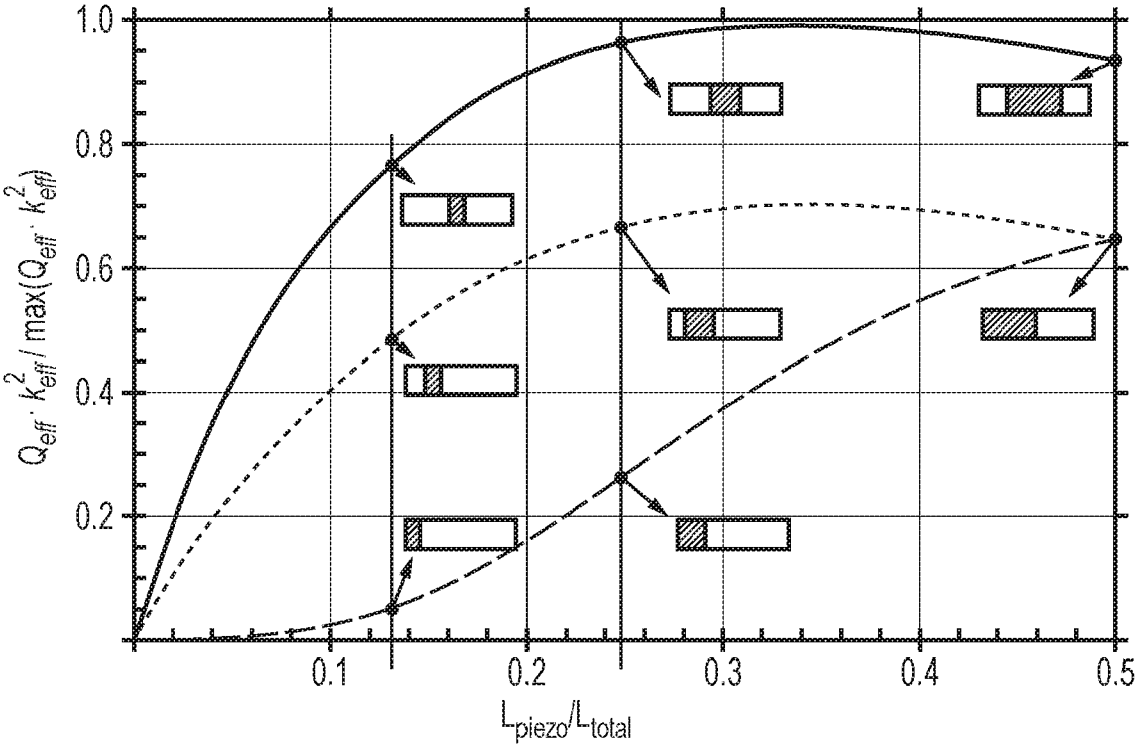

1.0
0.8
0.6
0.4
0.2
0.1
0.2
0.3
0.4
0.5
$Q_{eff} \cdot k_{eff}^2 / \max(Q_{eff} \cdot k_{eff}^2)$
L_{piezo}/L_{total}

FIG. 6B

28 10 22

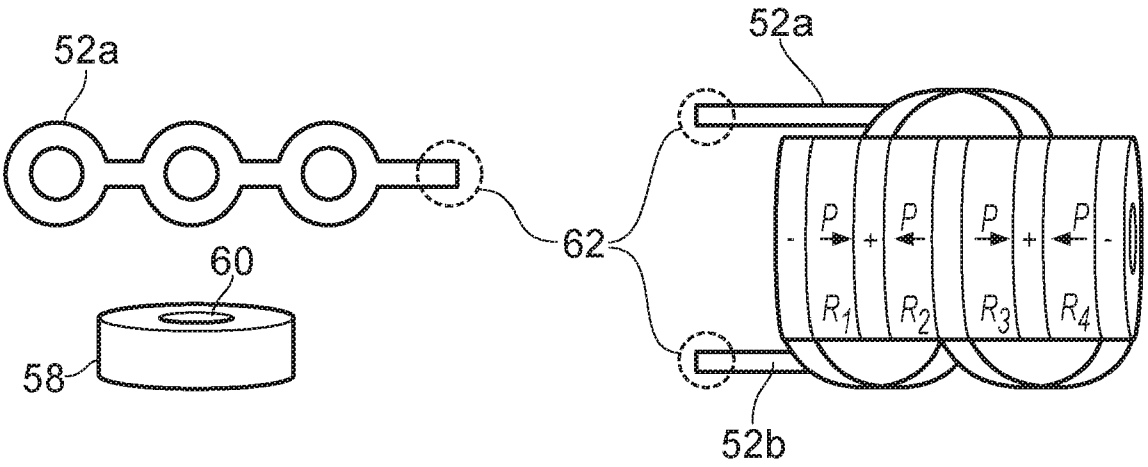


FIG. 7

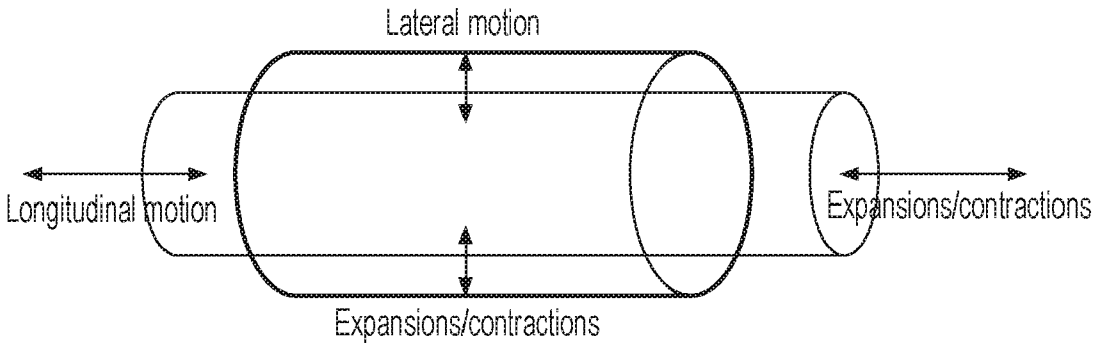


FIG. 8

28 10 22

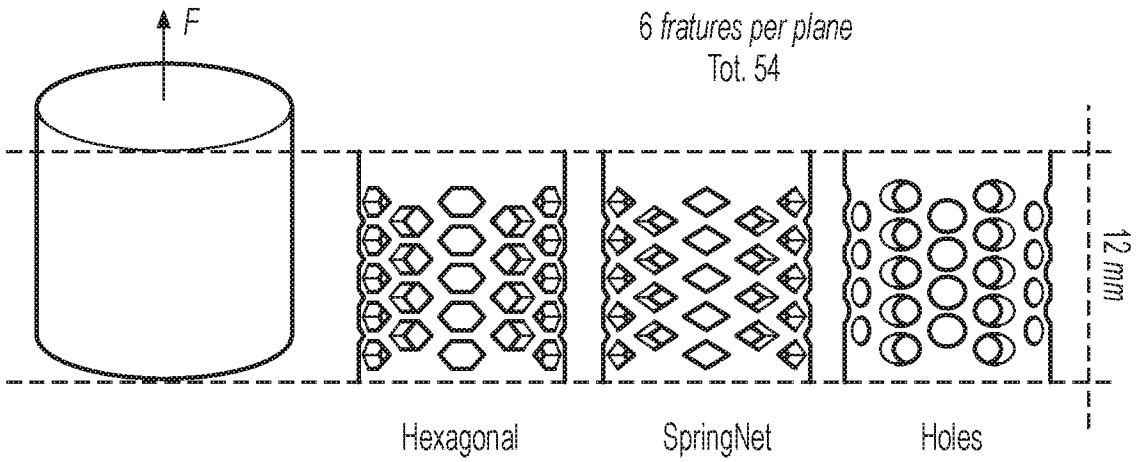


FIG. 9

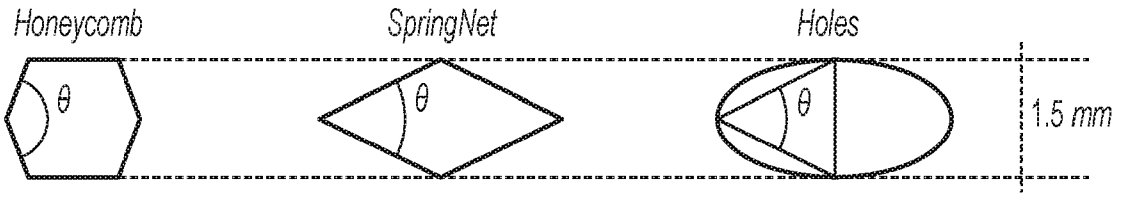


FIG. 10

28 10 22

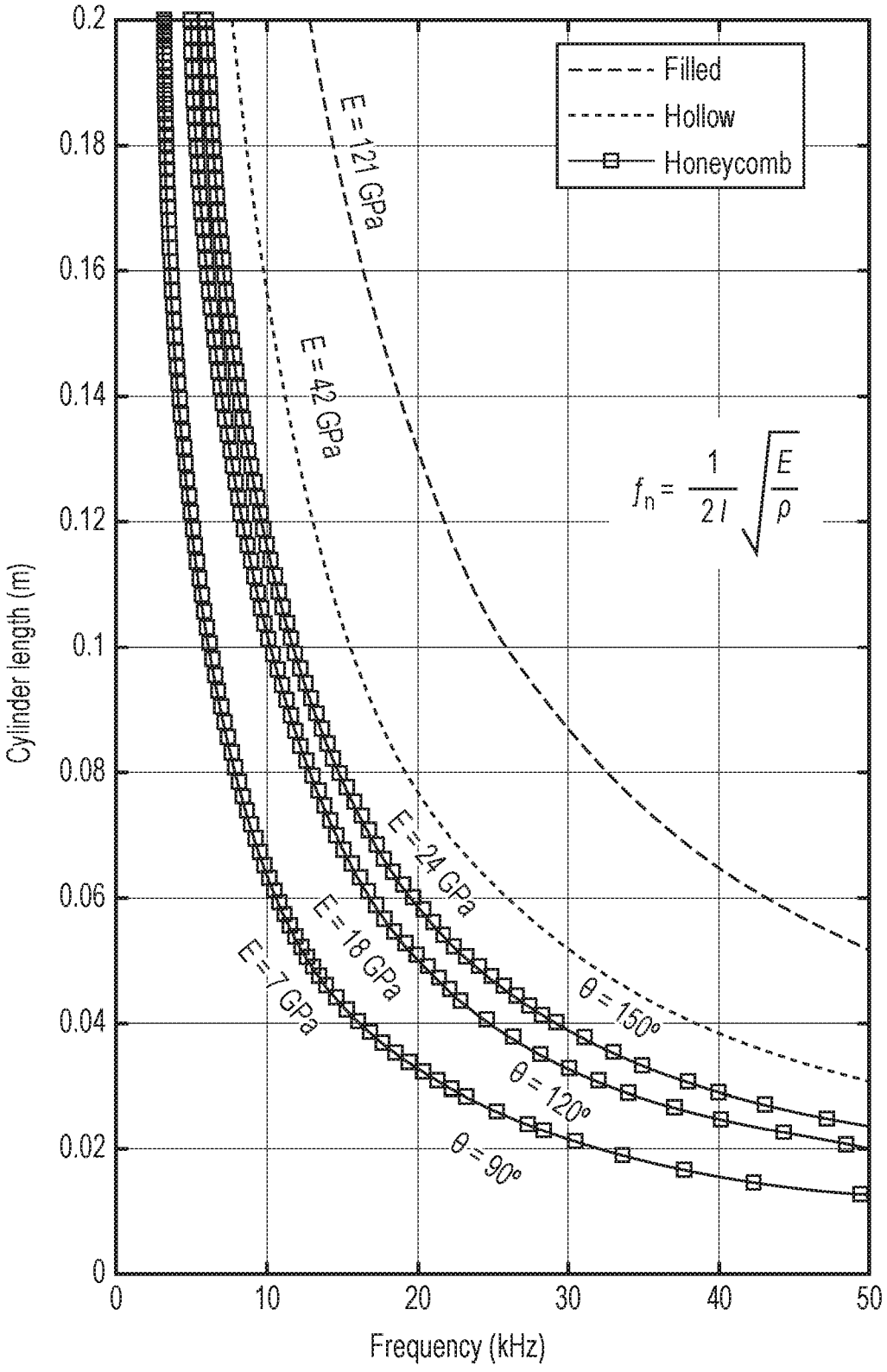


FIG. 11

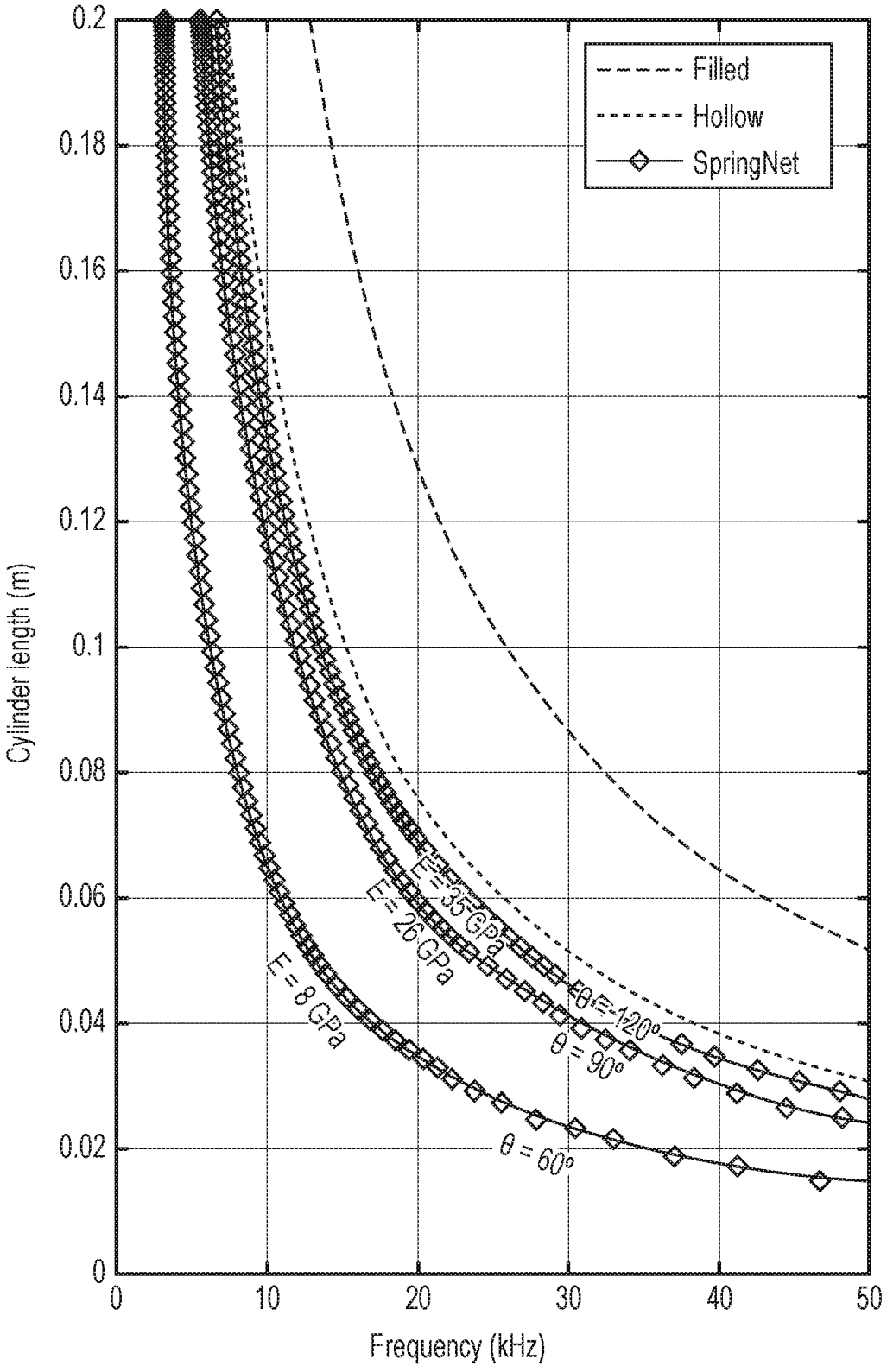

Filled
Hollow
SpringNet
Cylinder length (m)
Frequency (kHz)
0.2
0.18
0.16
0.14
0.12
0.1
0.08
0.06
0.04
0.02
0
0
10
20
30
40
50
E = 35 GPa
E = 26 GPa
E = 8 GPa
θ = 120°
θ = 90°
θ = 60°

FIG. 12

28 10 22

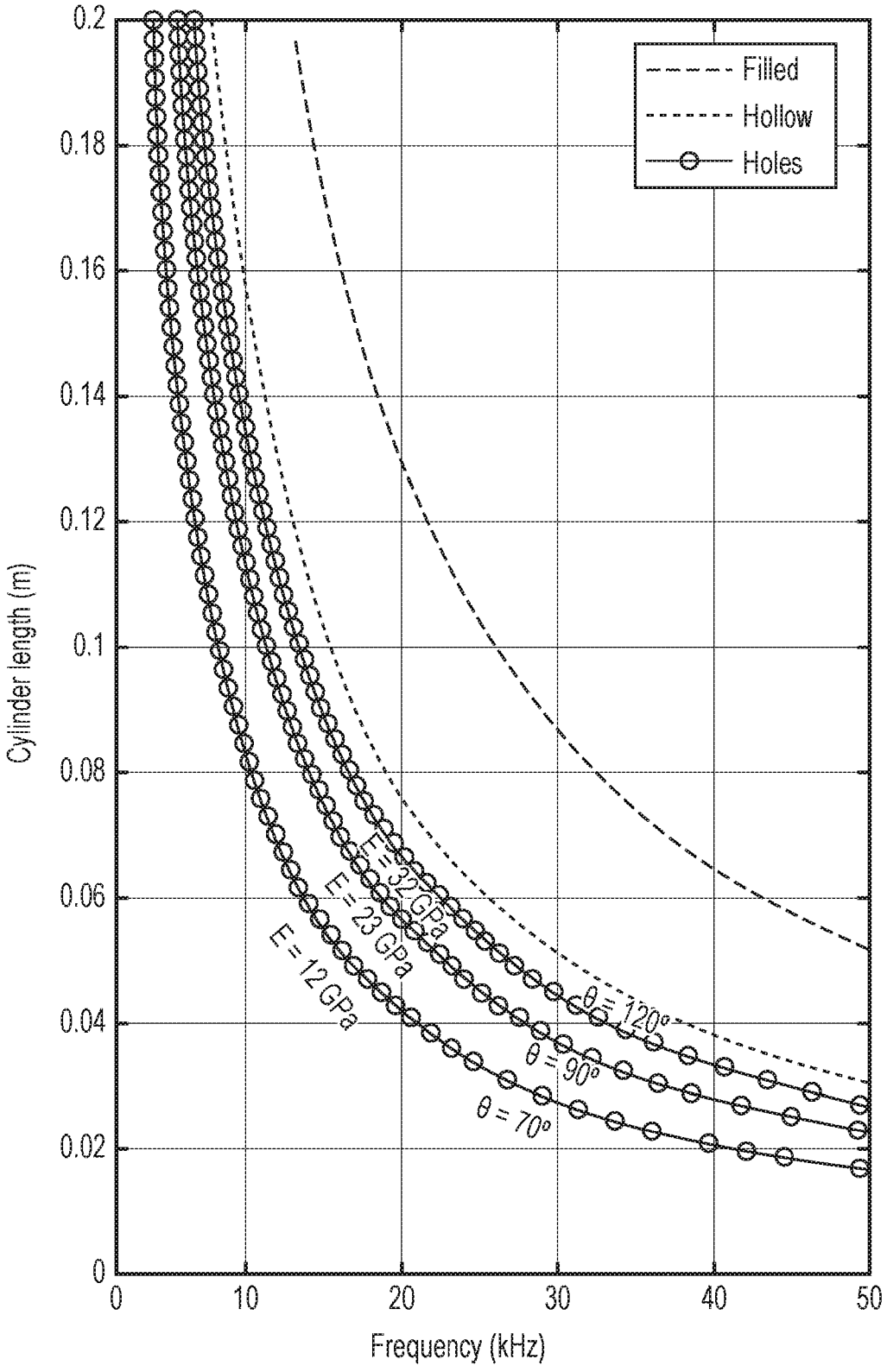


FIG. 13

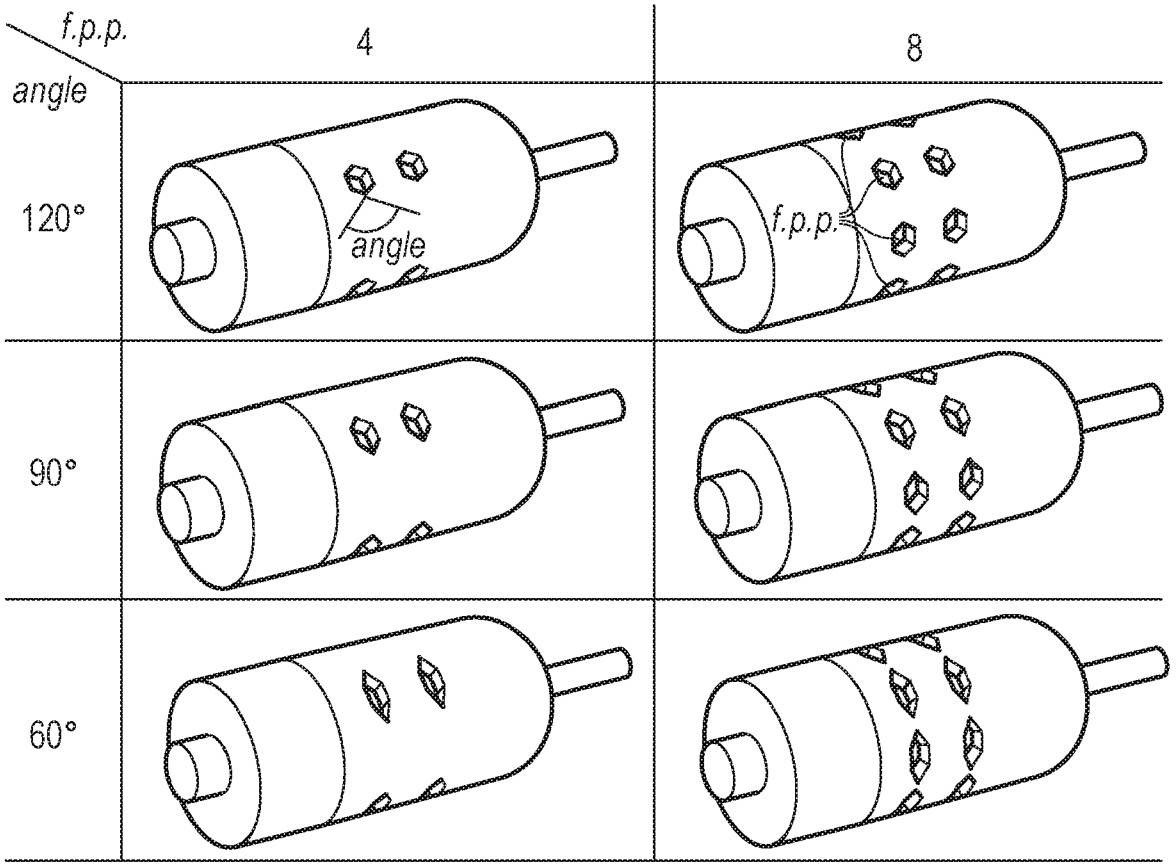


FIG. 14

28 10 22

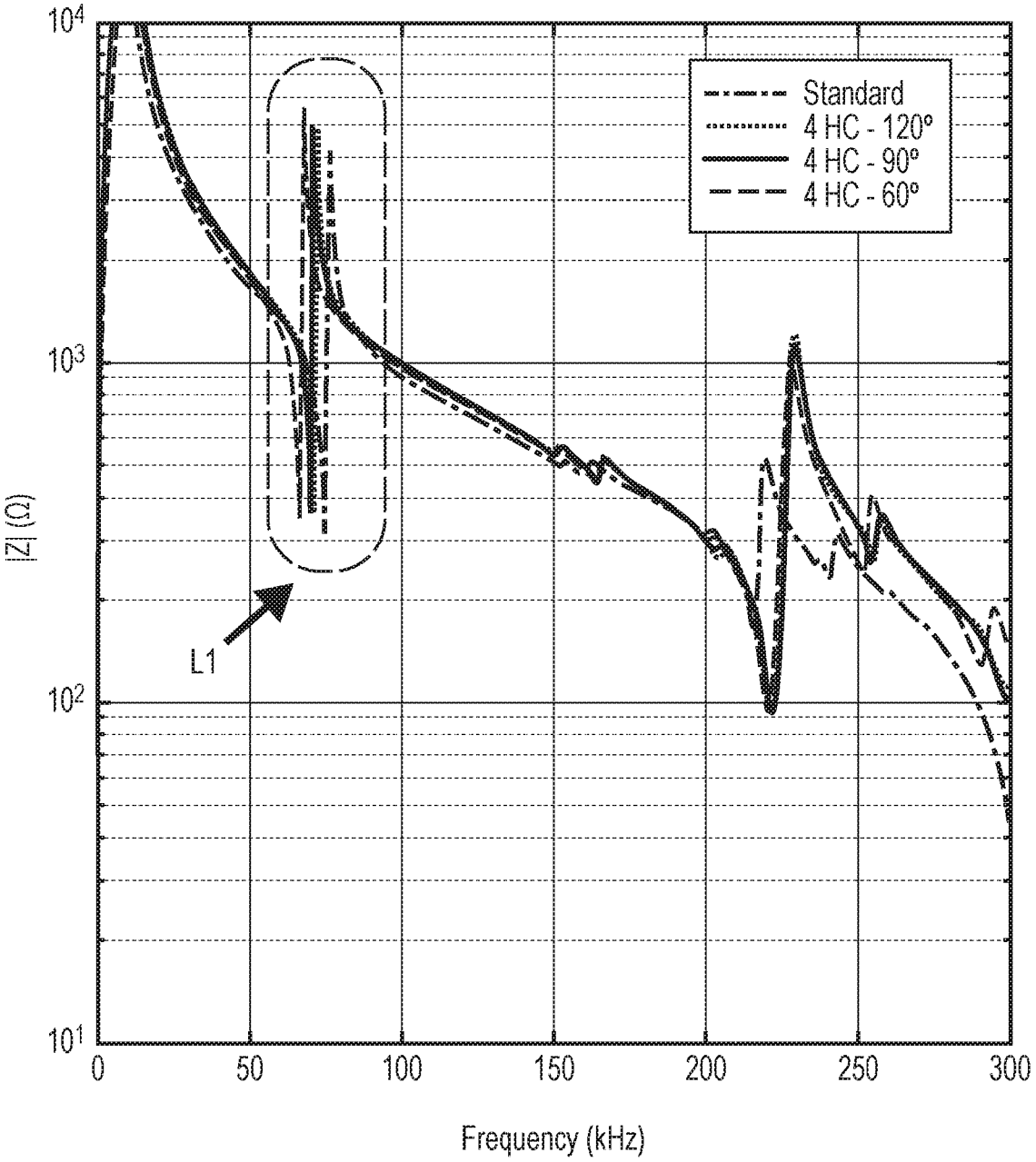


FIG. 15

28 10 22

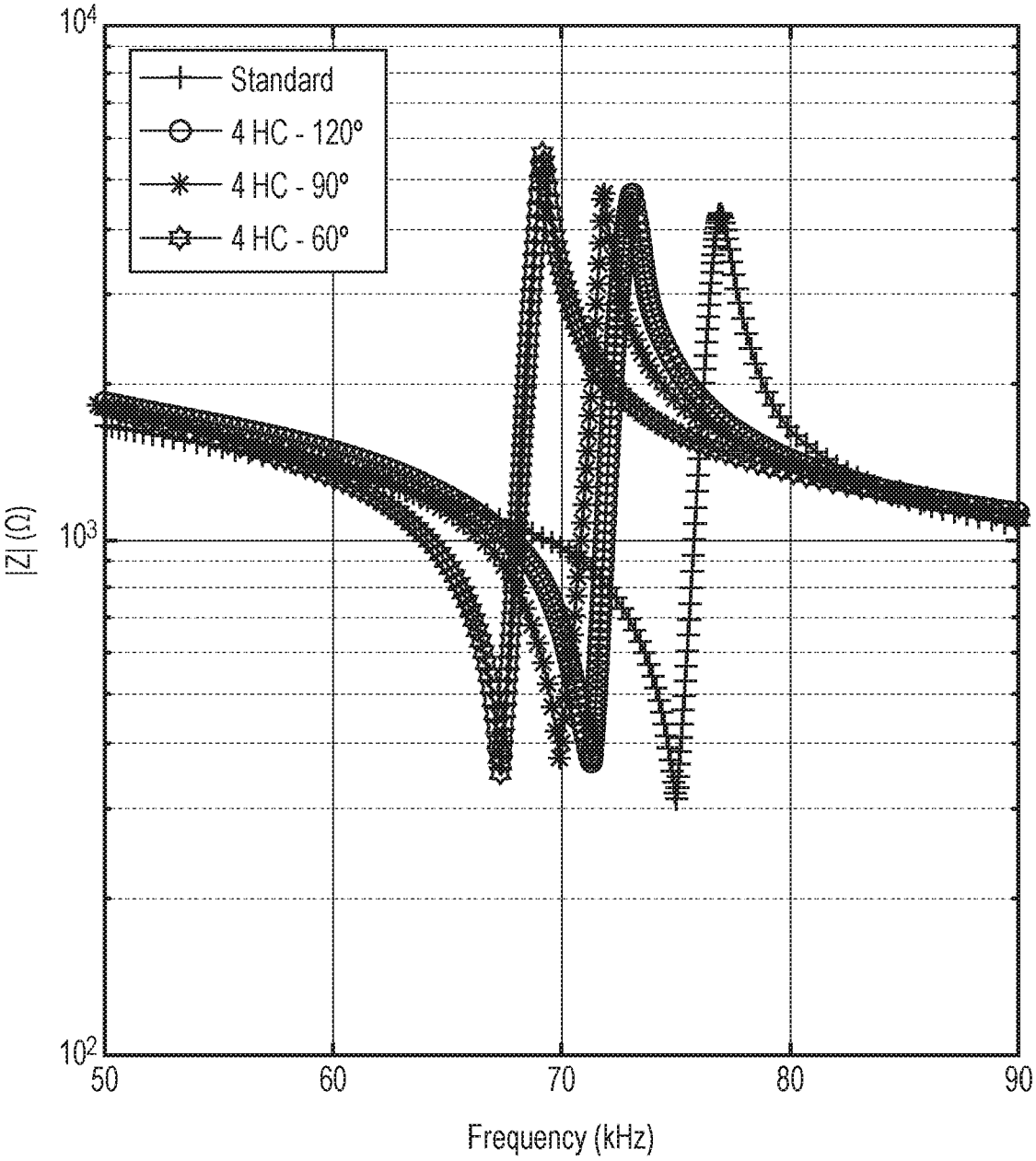


FIG. 16

28 10 22

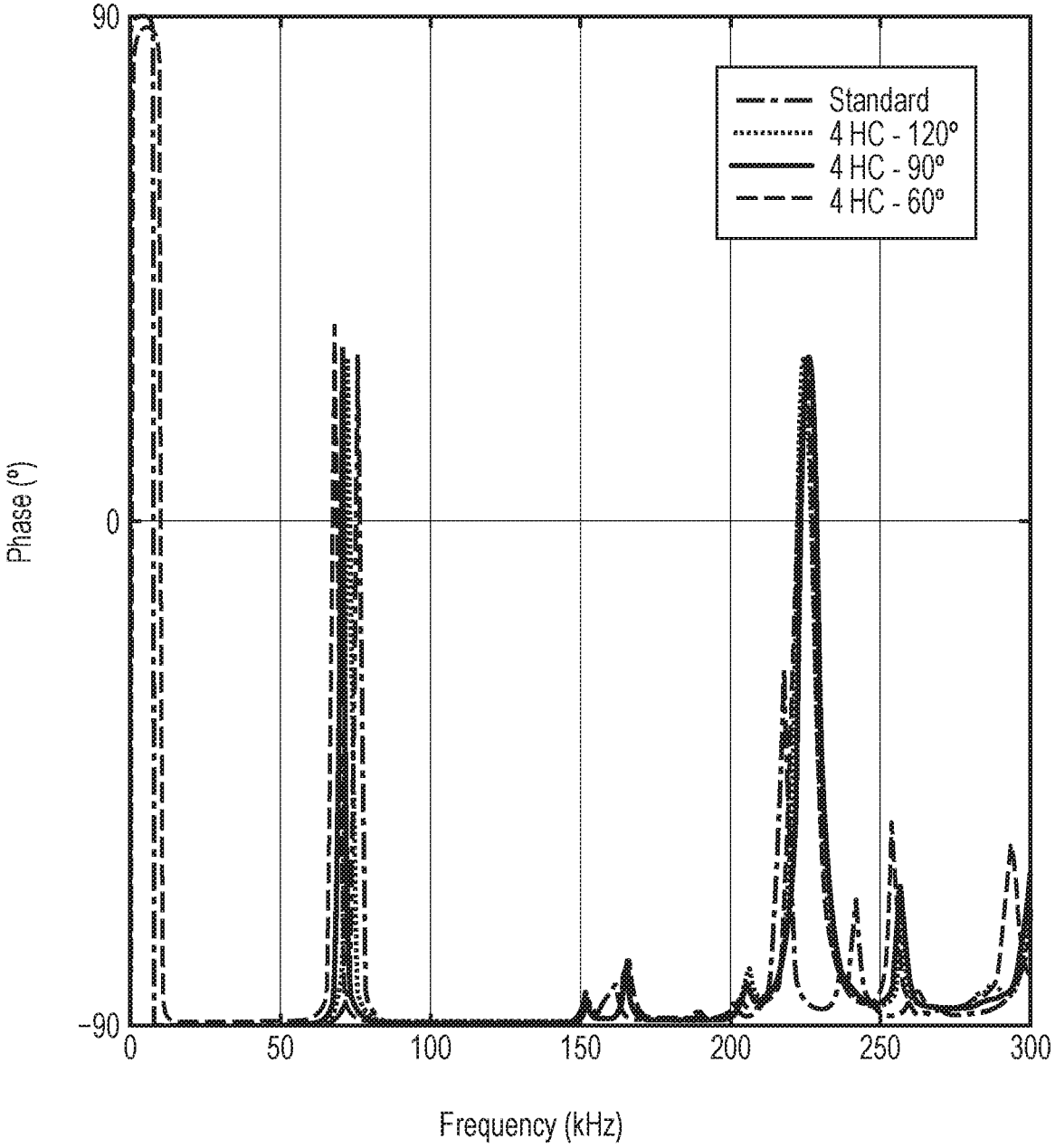


FIG. 17

28 10 22

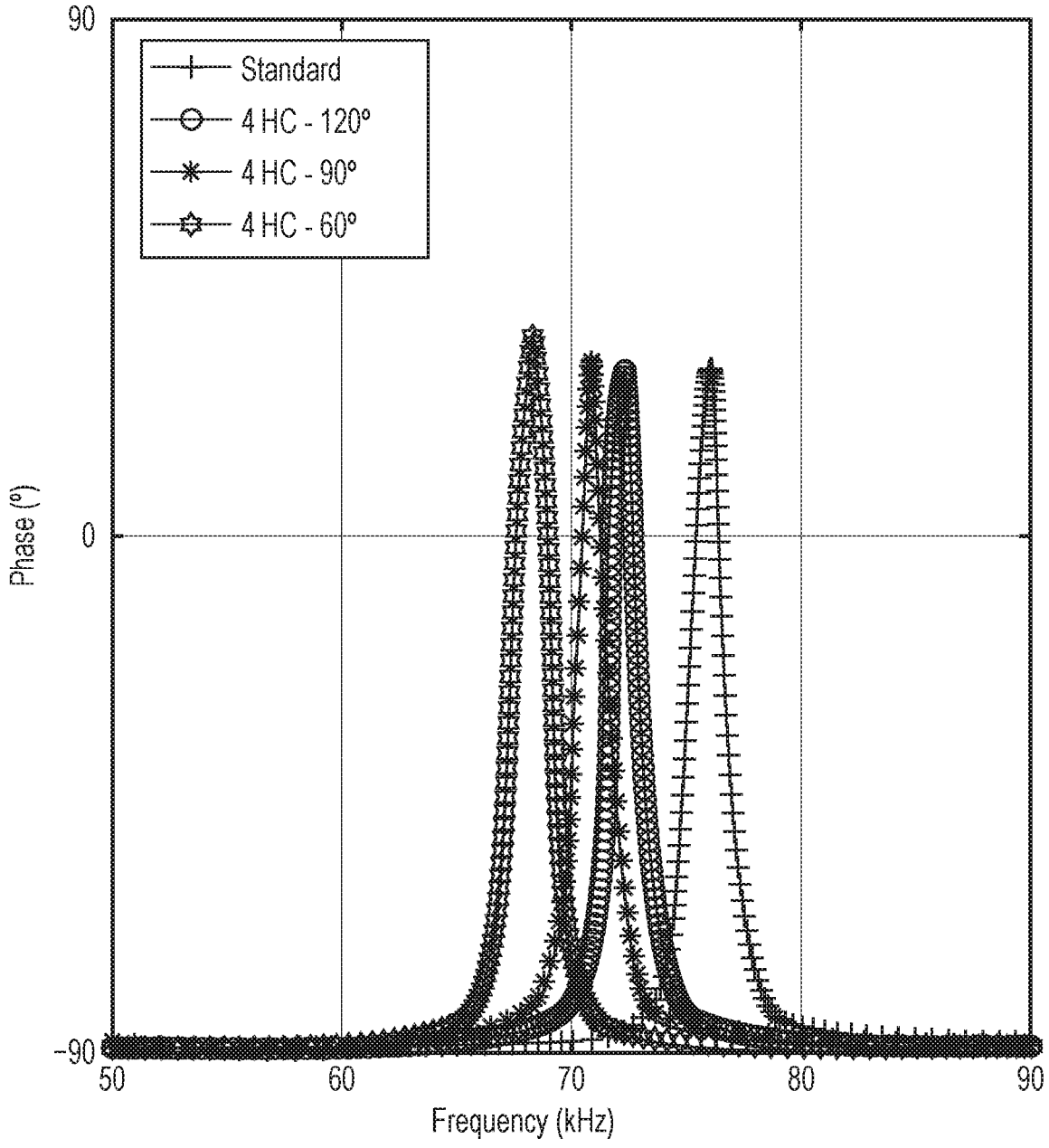


FIG. 18

28 10 22

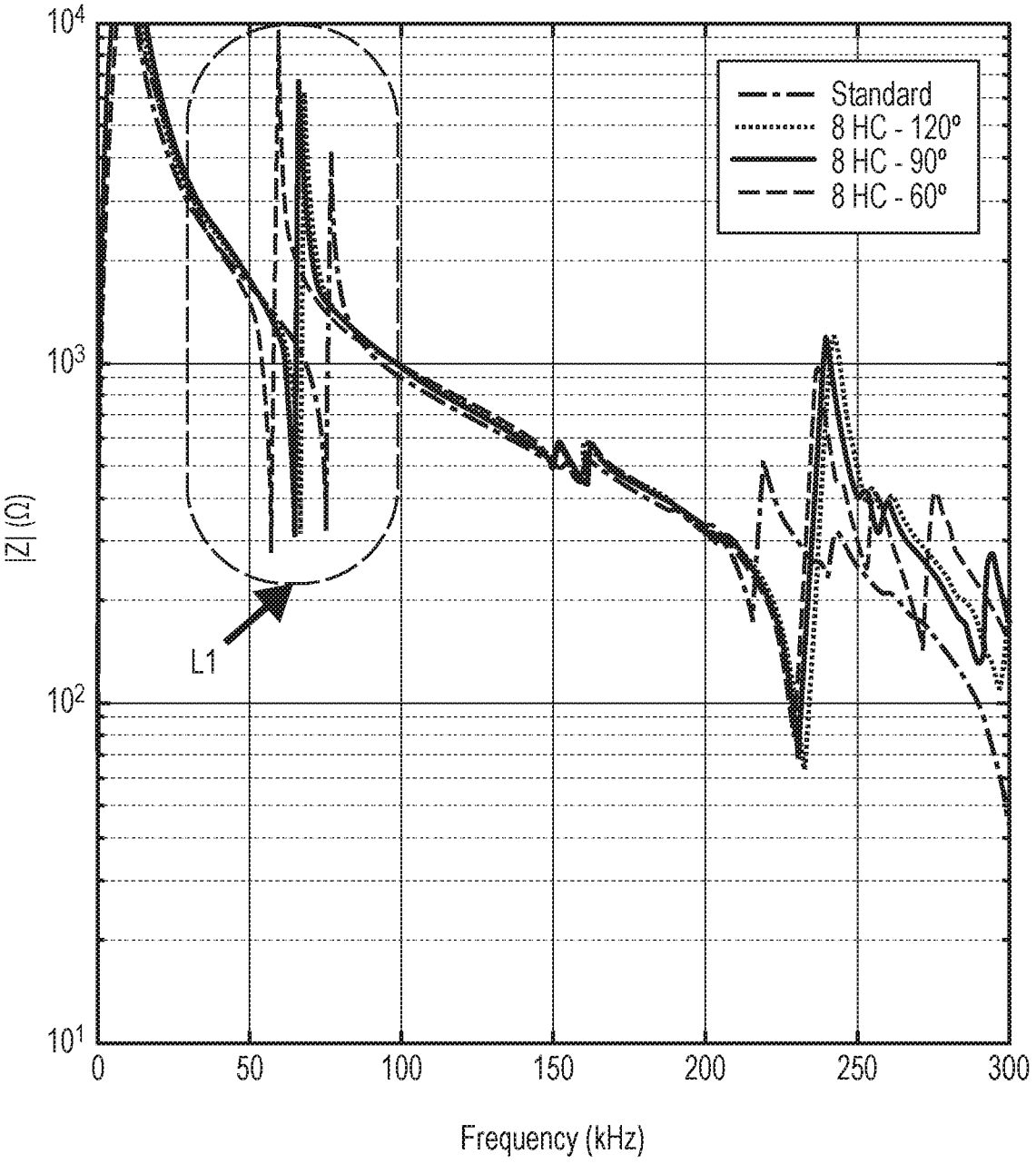


FIG. 19

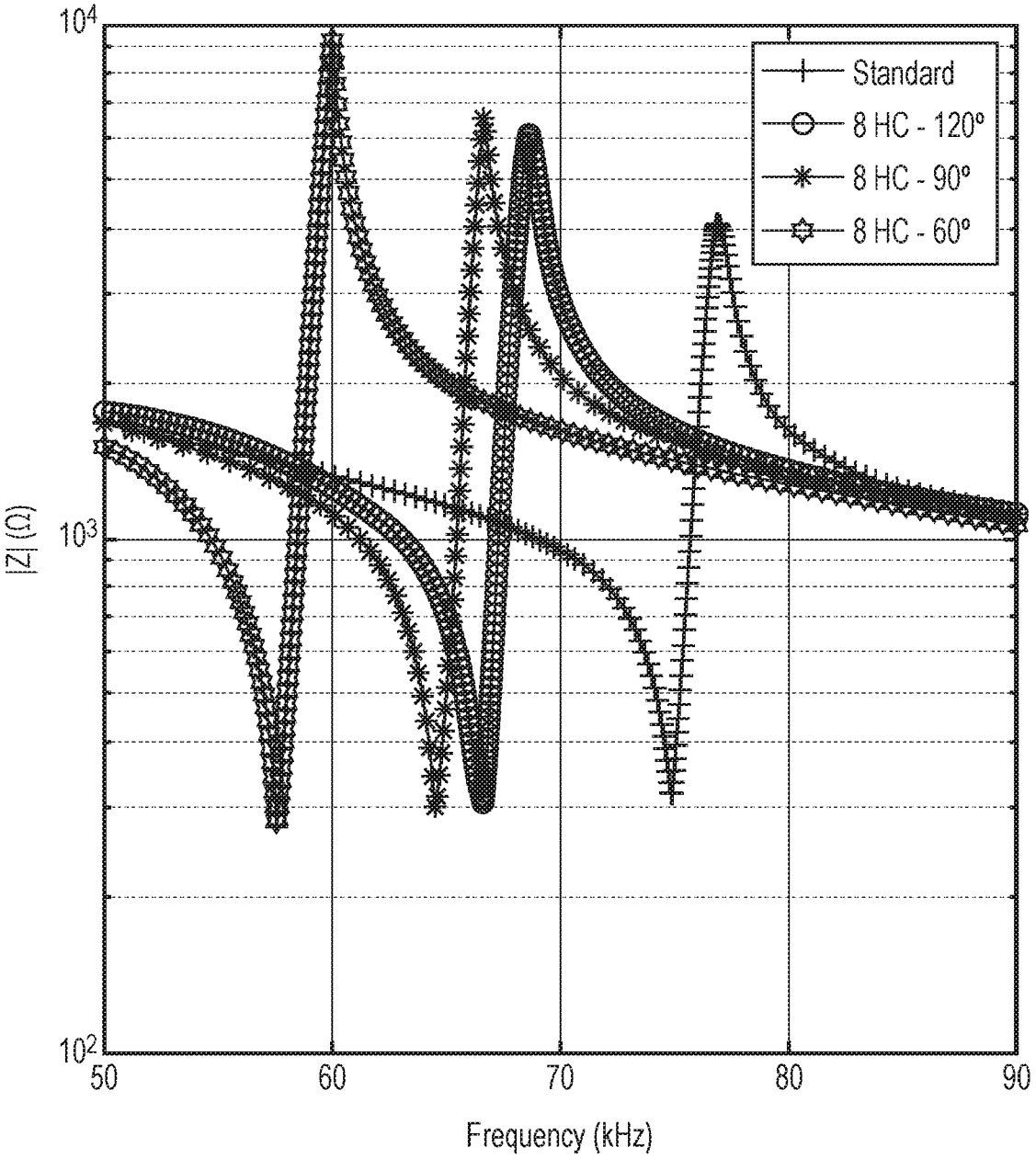

10^4
10^3
10^2
|Z| (Ω)
50
60
70
80
90
Frequency (kHz)
Standard
8 HC - 120°
8 HC - 90°
8 HC - 60°

FIG. 20

28 10 22

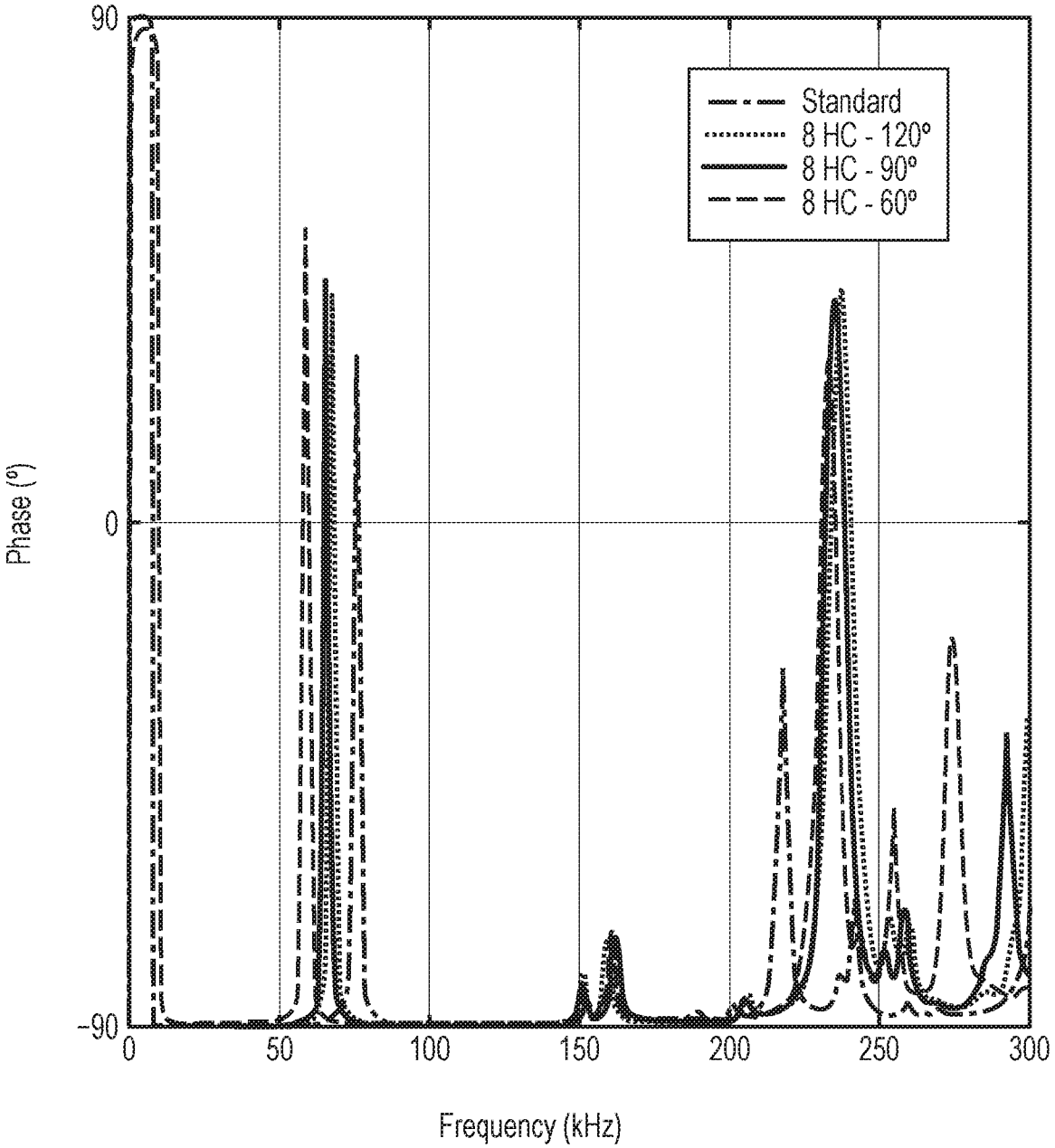


FIG. 21

28 10 22

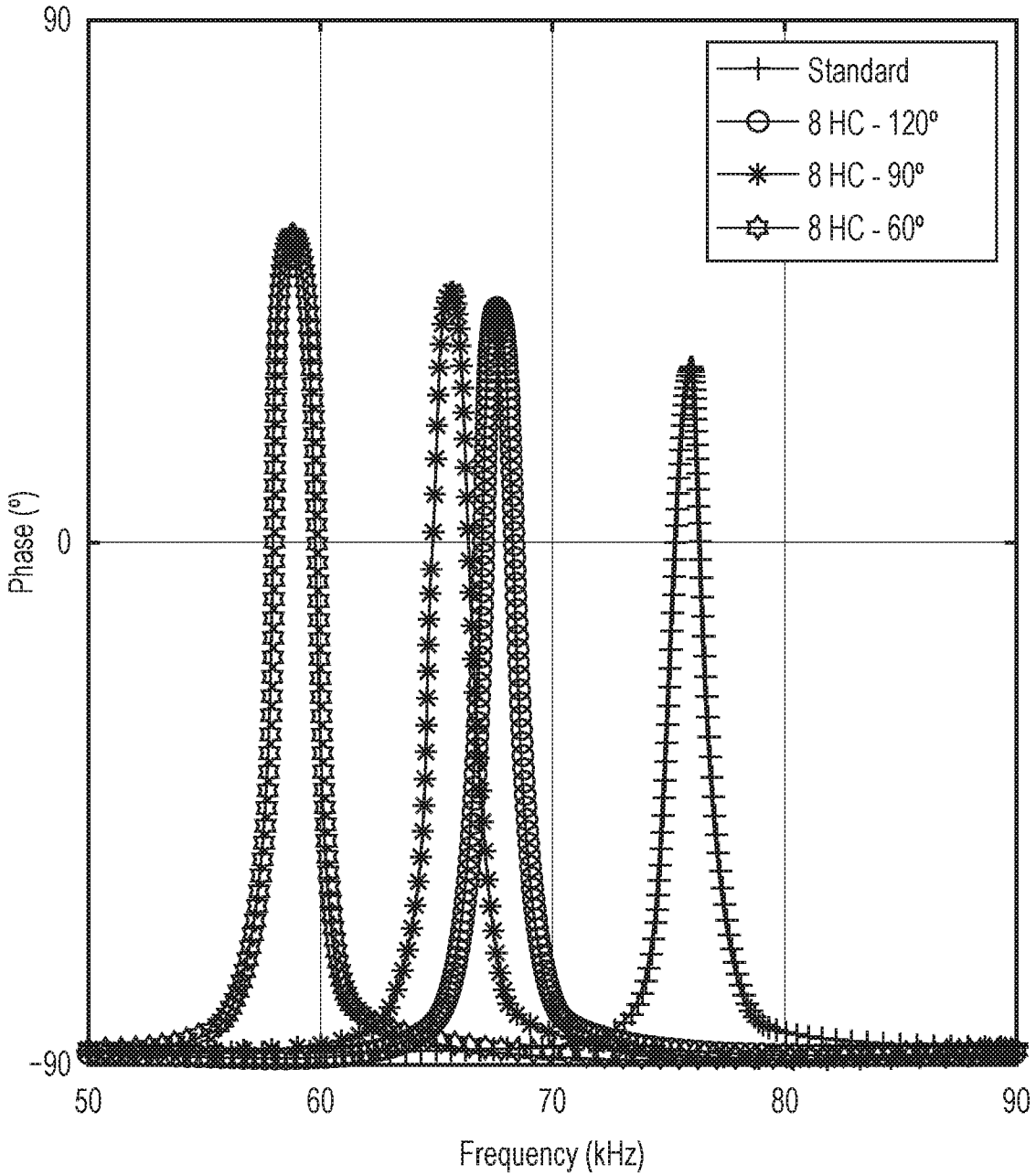


FIG. 22

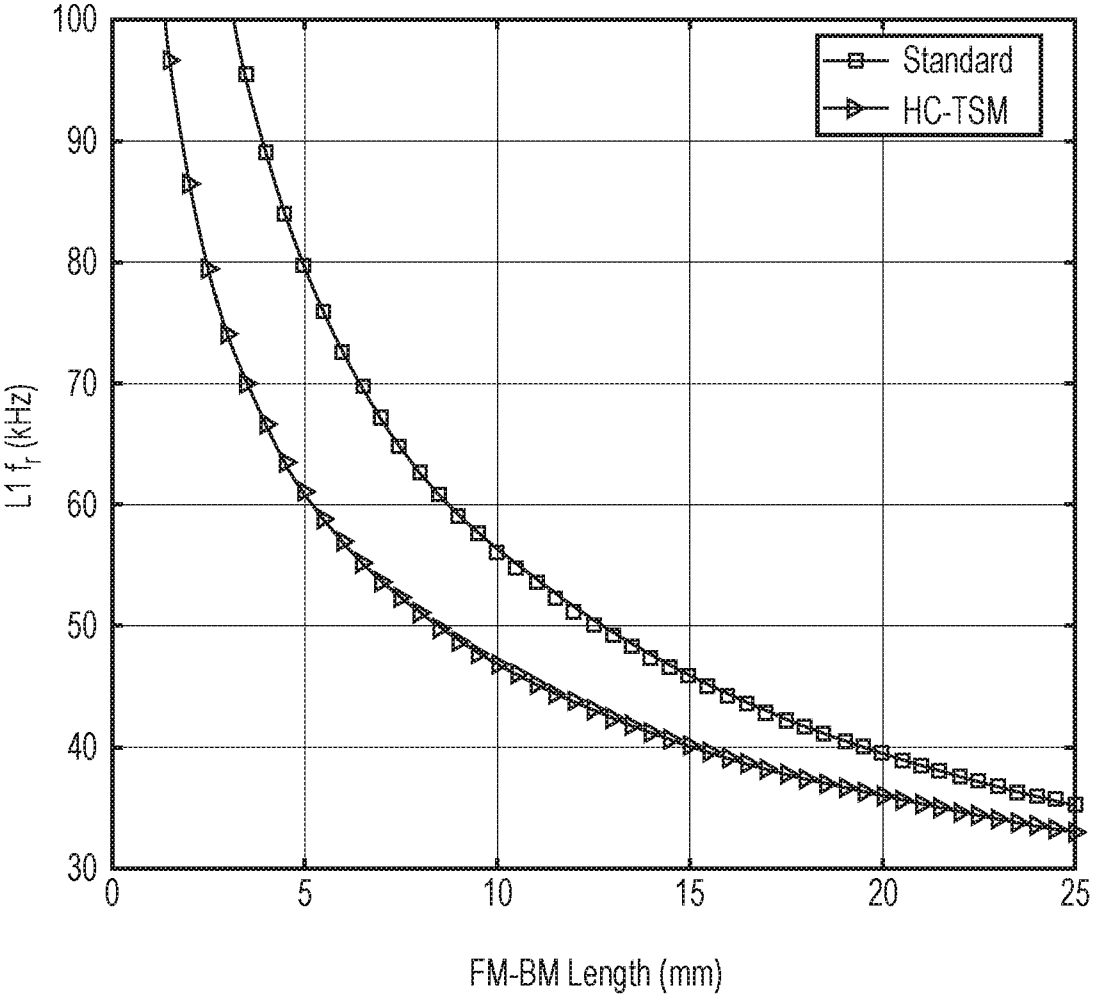

100
90
80
70
60
50
40
30
0
5
10
15
20
25
L1 f_r (kHz)
FM-BM Length (mm)
Standard
HC-TSM

FIG. 23

28 10 22

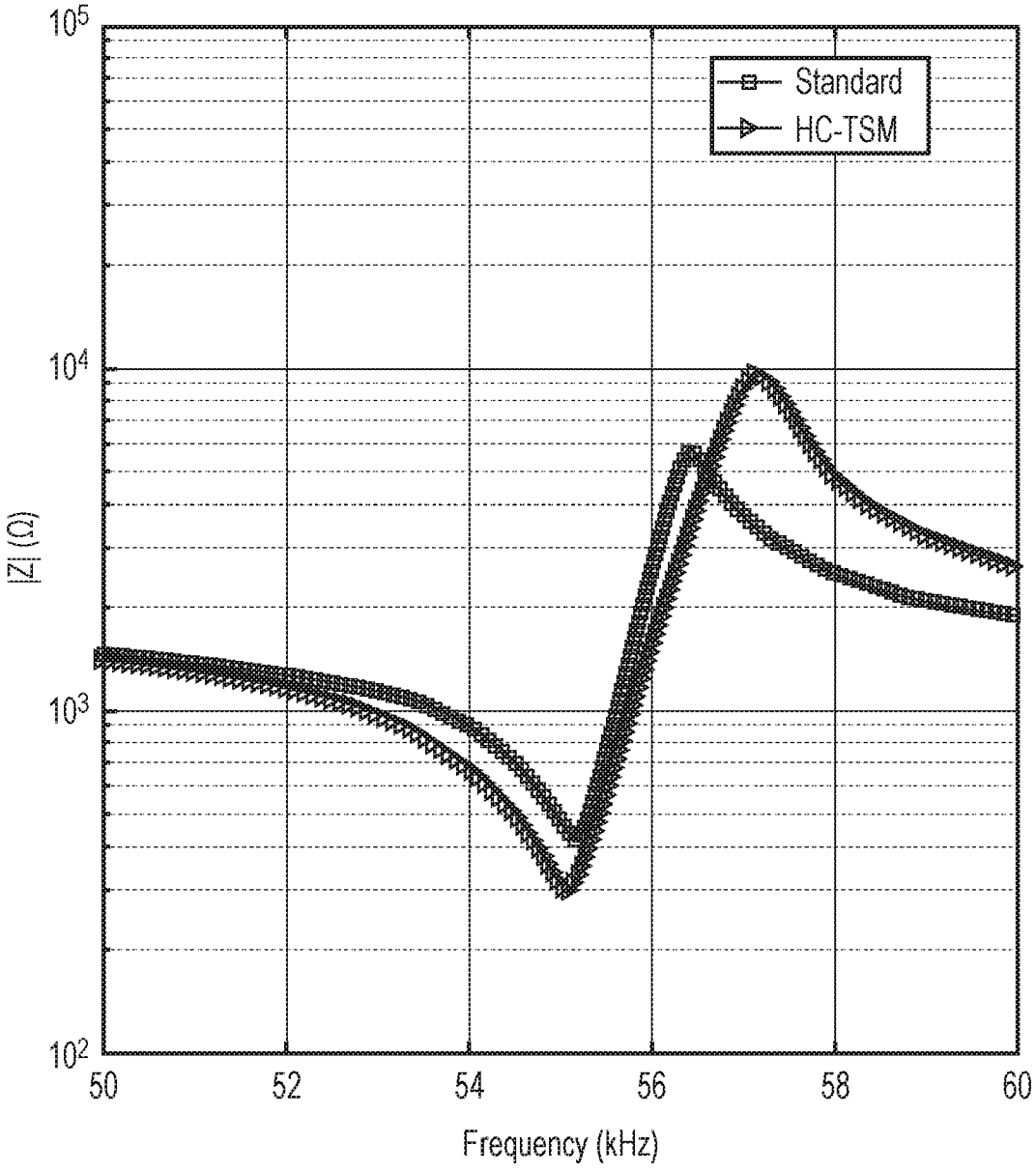


FIG. 24

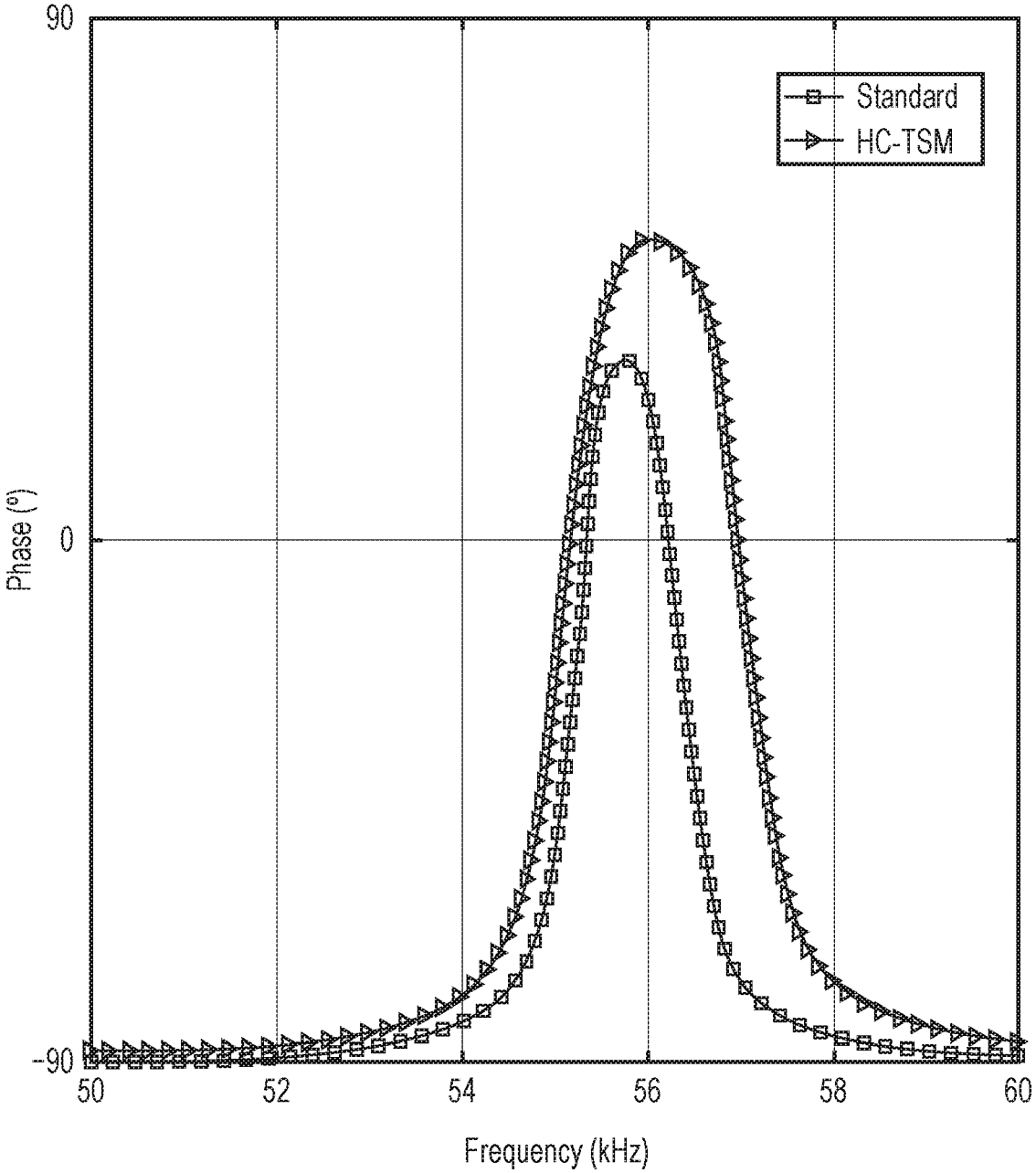


FIG. 25

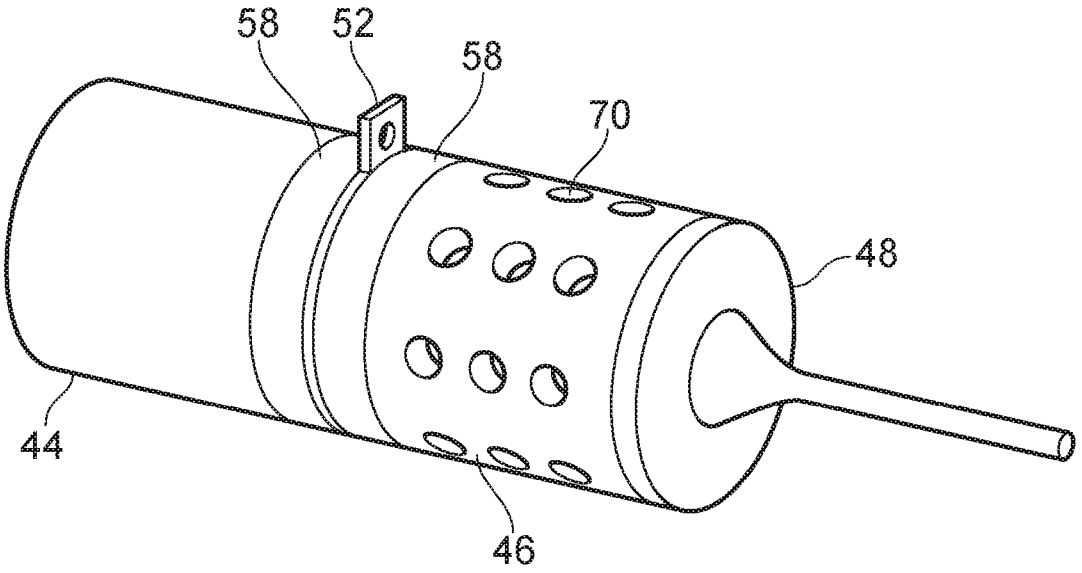


FIG. 26

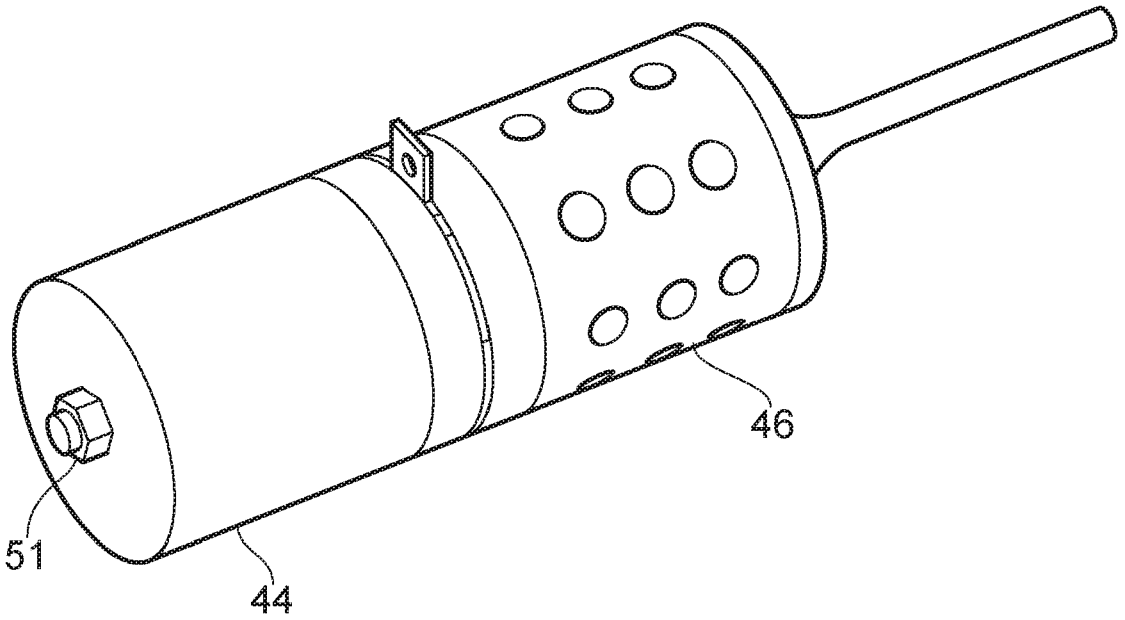


FIG. 27

28 10 22

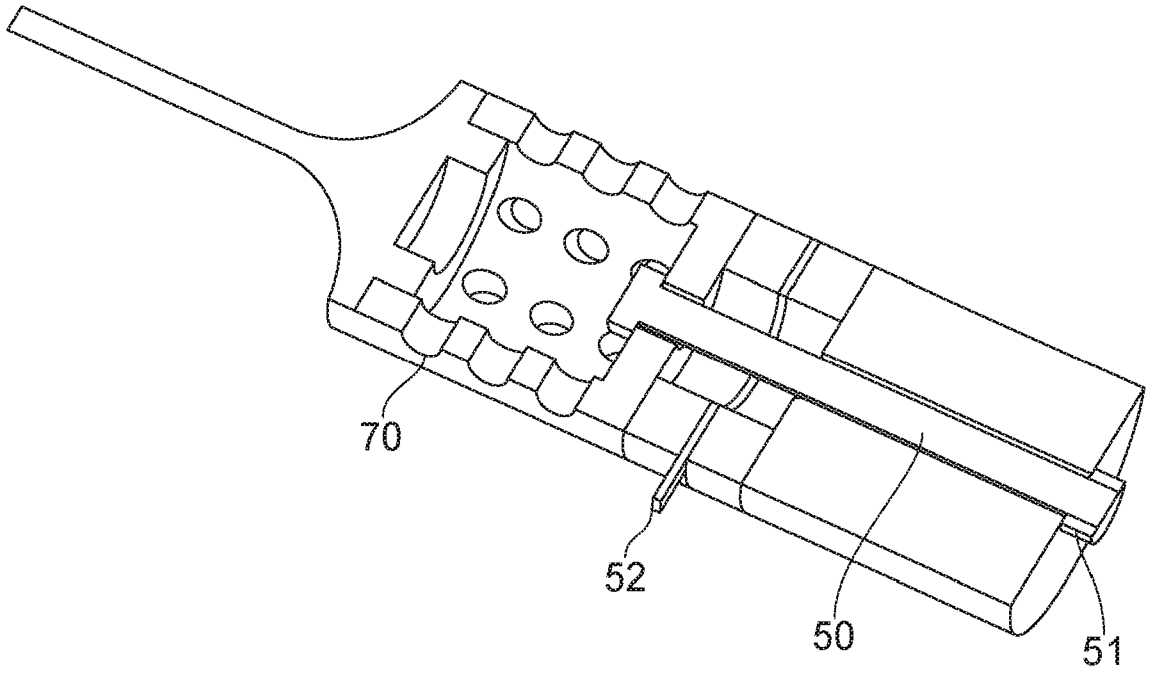


FIG. 28

28 10 22

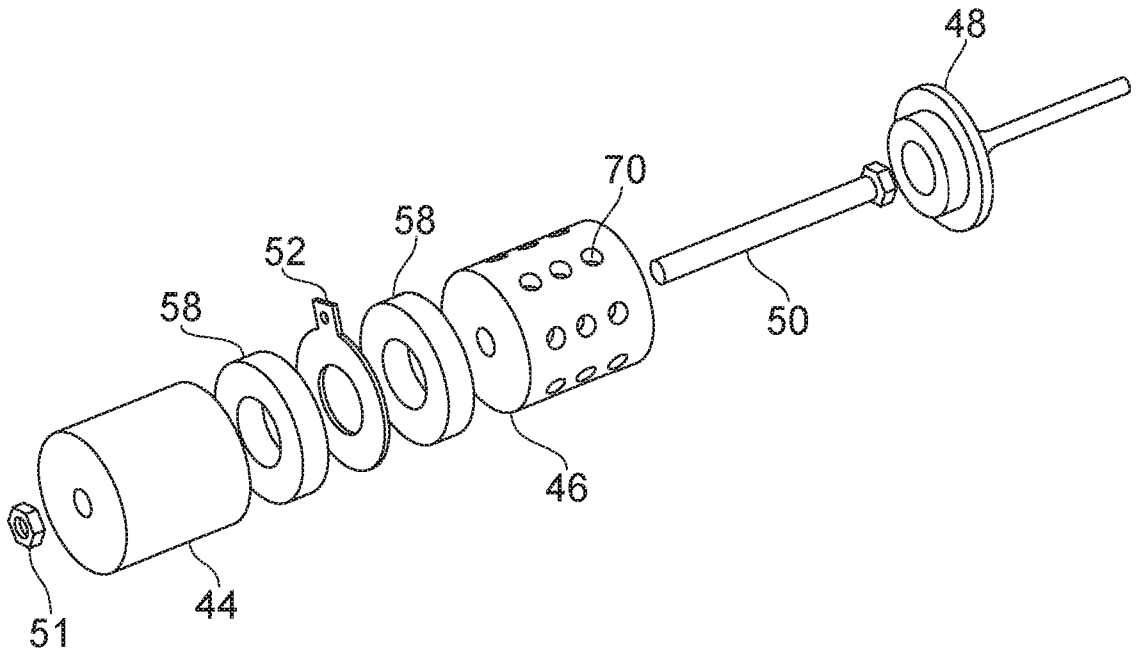


FIG. 29

28 10 22

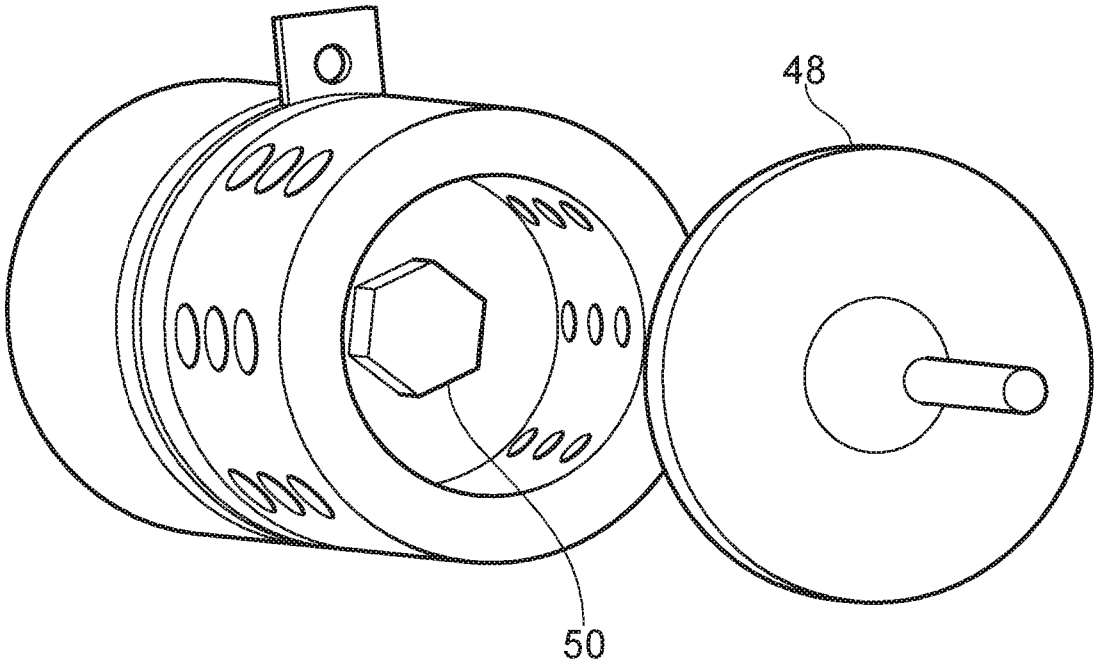


FIG. 30

28 10 22

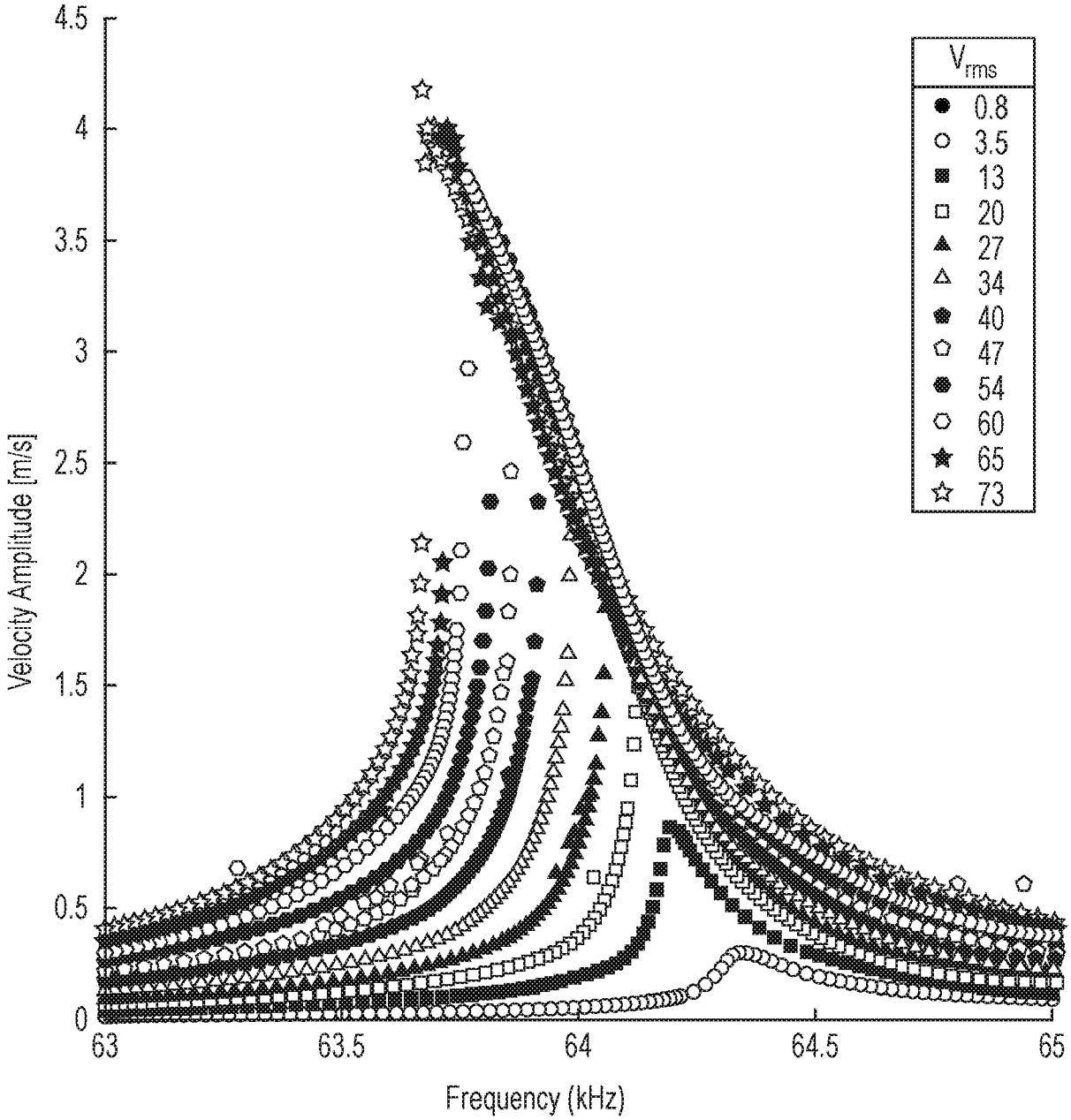


FIG. 31

28 10 22

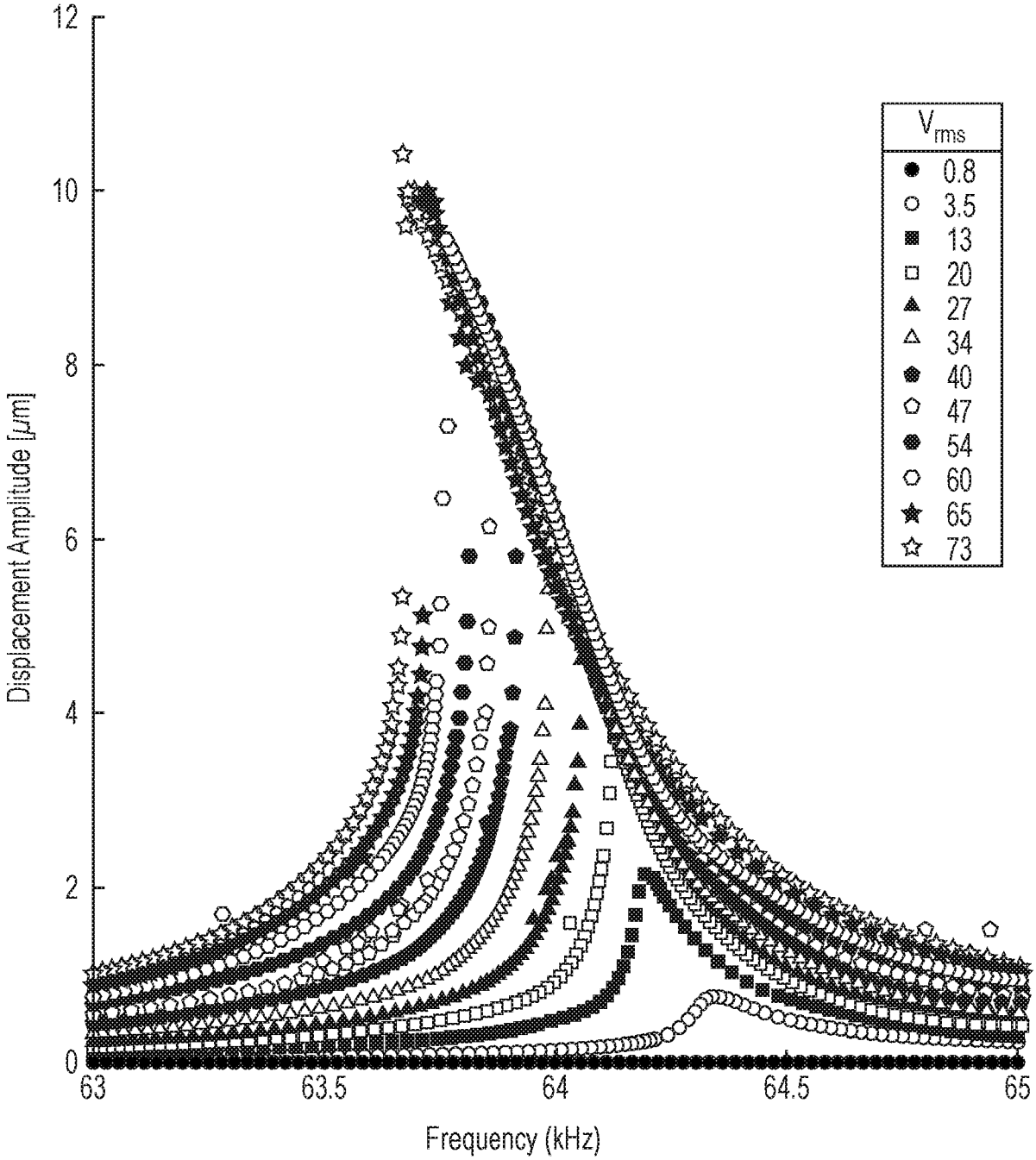


FIG. 32

ULTRASONIC TRANSDUCER

Field of the Invention

The present invention relates to an ultrasonic transducer and to a method of operation of an ultrasonic transducer. Such an ultrasonic transducer is of particular, although not necessarily exclusive, interest for surgical applications.

Background

The designs of modern ultrasonic surgical devices either for hard or soft tissue almost always resemble the configuration invented by Paul Langevin and Chilowsky in 1922 for underwater applications [1]. Generally, these devices adopt ultrasonic vibrations to enhance cutting performance, employing a transducer mounted in a hand-held device. In the case of soft tissue cutting some common features can be identified. Fig. 1 shows the Harmonic® ACE® + Shears (Ethicon® Endosurgery, Johnson & Johnson, Cincinnati, Ohio, USA), where the waveguide 10, handpiece 12 and Langevin transducer 14 can be recognised. The inset in Fig. 1 also shows the vibration direction "Vib", longitudinal in this case (parallel to the longitudinal axis of the transducer and waveguide), and the jaw-blade mechanism comprising a pivotable jaw 16 and the vibrating blade 18.

The Harmonic® ACE® + Shears together with the SENHANCE™ Ultrasonic (BOWA® Medical, BOWA-electronic GmbH & Co. KG, Gomaringen, Germany) represent the only two ultrasonic cutting devices compatible with robotic surgery platforms at the time of writing, those platforms, respectively, the Da Vinci® Surgical System (Intuitive® Surgical Inc., Sunnyvale, California, USA) and the SENHANCE™ Surgical System (BOWA® Medical, Gomaringen, Germany).

One of the most recent inventions for Da Vinci® energy instruments is the EndoWrist® (Intuitive® Surgical Inc.). This articulated joint enables a range of motions at the end effector similar to that of the human wrist, thus replicating the experience of open surgery. Fig. 2 shows a generic Da Vinci® end-effector with EndoWrist® technology. The end-effector 20 is attached at the end of shaft 22 and has first pivot joint 24 permitting flexion and extension (rotation about a first axis) and a second pivot joint 26 permitting adduction and abduction (rotation about a second axis, orthogonal (in this case) with respect to the first axis). A grasping tool 28 is disposed at the distal end of the end-effector.

Several energy instruments are available at the time of writing with EndoWrist® technology, of 5-10 mm in diameter, which allows them to be inserted through a laparoscopic port and manoeuvred inside the human body. To date, an ultrasonic cutting device with EndoWrist® technology does not exist. Fig. 2 shows the range of motions available for an EndoWrist® generic end-effector [2].

In current ultrasonic cutting devices, only axial and rotation movements are permitted, as the transducers are too large to fit through the 5-10 mm trocar. The transducer is axially constrained to the robotic arm

and the waveguide, which transfers the ultrasonic vibration from outside the human body to the end effector inside, cannot be bent. This represents a significant disadvantage for surgical ultrasonic devices. In fact, although ultrasonic cutting has shown to be more precise and effective than other energy instruments, and with excellent coagulation speed, the latter are still preferred due to their dexterity.

US 9,408,622 B2 discloses a bendable waveguide that addresses some of the problems identified above but still provides only limited dexterity.

Ultrasonically-actuated surgical tools are an alternative to electrocautery tools, with the potential to avoid some of the disadvantages of electrocautery tools, whilst achieving similar outcomes.

The Harmonic® ACE + Shears is the only ultrasonic device compatible with the Da Vinci® Surgical System. One of its main drawbacks is the lack of flexibility, as it is not compatible with EndoWrist®. The main reason for this is the size of the ultrasonic transducer which is too long and large to be clamped at the end of an end-effector wristed joint to fit through a burr hole or laparoscopic port.

Long rigid waveguides are preferred to transfer the vibrational energy at ultrasonic frequencies from outside to inside the human body. This, inevitably, limits ultrasonic energy instruments to a few applications not? requiring accessibility to difficult sites.

Table 1 outlines the advantages and disadvantages of ultrasonic cutting instruments compared with monopolar and bipolar surgical tools for minimally invasive surgery. Despite the numerous advantages reported in Table 5.1, the lack of flexibility of the device in terms of manoeuvrability limits its application in several procedures as only axial targets can be reached, due to the long straight waveguide and the lack of articulated joints at the blade tip.

Table 1: Advantages and disadvantages of ultrasonic energy instruments compared with monopolar and bipolar electrocautery surgical tools for minimally invasive surgery [6], [7].

Advantages of ultrasonic surgical tools for soft tissue	**Disadvantages of ultrasonic surgical tools for soft tissue**
• Decreased thermal spread. • Reduced coagulum. • Minimal collateral damage. • Multifunctionality of the instrument. • Cut and seal vessels up to 7 mm. • Less tissue sticking to the instrument. • No stray energy. • No neuromuscular stimulation.	• Smoke formation while cutting. • Lack of flexibility, not compatible with EndoWrist®. • Surrounding damage when used in reduced space, difficult to manoeuvre. • Temperature of the shaft (>190 °C).

Advantages of ultrasonic surgical tools for soft tissue	Disadvantages of ultrasonic surgical tools for soft tissue
• No electrical energy through the patient. • Can be sterilised. • Superior cutting precision. • Reduced procedure time.	

Ultrasonic technology is adopted in robotic abdominal laparoscopic surgery for parenchymal (functional tissue) transections where the parenchyma of an organ is dissected from connective and supporting tissue. Ultrasonic energy is also used in lobectomy procedures for the removal of a part of an organ. Other common laparoscopic procedures where ultrasonic energy is preferred, despite the unarticulated instrument, include gastrectomy, adrenalectomy, splenectomy and hepatectomy [6].

The present invention has been devised in light of the above considerations.

Summary of the Invention

With current state-of the-art technology of Langevin transducer design, miniaturisation of an ultrasonic surgical tool such as a dissector cannot be achieved while still preserving device functionality and performance.

Accordingly, the present inventors have addressed the issues identified above by considering in detail the effect of the mechanical compliance of the components of a transducer along the vibrational energy transfer path of the transducer.

In a first aspect, the present invention provides an ultrasonic transducer for surgical applications, the ultrasonic transducer comprising:
a back mass;
a front mass;
an ultrasonic actuator arrangement held between the back mass and the front mass;
an ultrasonic horn arrangement forward of the front mass,
wherein vibrations generated by the ultrasonic actuator arrangement are conducted into the front mass and into the ultrasonic horn arrangement along a vibrational energy transfer path and are amplitude amplified by the ultrasonic horn arrangement,
and wherein one or more of the back mass, front mass and ultrasonic horn arrangement includes a plurality of openings intersecting the vibrational energy transfer path and configured to provide an increased mechanical compliance in a direction along the vibrational energy transfer path.

In a second aspect, the present invention provides a surgical tool comprising an ultrasonic transducer according to the first aspect.

In a third aspect, the present invention provides a method of operation of an ultrasonic transducer, the ultrasonic transducer comprising:
a back mass;
a front mass;
an ultrasonic actuator arrangement held between the back mass and the front mass;
an ultrasonic horn arrangement forward of the front mass,
the method including applying an electrical signal to the ultrasonic actuator arrangement to generate vibrations to be conducted into the front mass and into the ultrasonic horn arrangement along a vibrational energy transfer path and amplitude amplified by the ultrasonic horn arrangement,
wherein one or more of the back mass, front mass and ultrasonic horn arrangement includes a plurality of openings intersecting the vibrational energy transfer path providing an increased mechanical compliance in a direction along the vibrational energy transfer path.

In a fourth aspect, the present invention provides a method of cutting tissue by ultrasonic cutting using an ultrasonic blade, including a method of operating of an ultrasonic transducer as set out in the third aspect and conducting the vibrational energy to the ultrasonic blade.

The transducer may be a Langevin type transducer, such as a bolted Langevin transducer. Such transducers are of interest for surgical applications due to their low frequency and high power operating characteristics.

The ultrasonic actuator arrangement may comprise a piezoelectric material element such as a piezoceramic element. A plurality of such elements may be provided. One or more associated electrodes may be provided in order to conduct a driving signal to the piezoelectric material element(s). Where the front and/or back mass is formed of an electrically conductive material such as metal, the front and/or back mass may provide ground electrical contact(s) for the piezoelectric material element(s).

The vibrational energy transfer path in the back mass, front mass and/or ultrasonic horn may include an annular portion. The annular portion may take the form of a hollow cylinder for example, with the wall of the cylinder extending along the vibrational energy transfer path and, in operation, vibrational energy passing along the wall of the cylinder. The plurality of openings intersecting the vibrational energy transfer path may therefore be provided through the wall of the annular portion. The openings are typically through-holes. Although it is possible in principle to use blind holes, the subsequent operation of the transducer is expected not to be as suitable.

Each opening may have a substantially uniform cross section along its depth. Considering the depth direction of the opening as the direction parallel to the walls of the opening, the depth direction may be substantially perpendicular to the vibrational energy transfer path (e.g. locally in the transducer).

The openings may each have the same size (e.g. the same diameter if the openings have circular cross sectional shape, or other characteristic linear dimension(s) for other shapes). The openings may have the same cross sectional area. Furthermore, the openings may have the same shape as each other, or may be selected from a limited number of shapes (e.g. two, three or four).

The openings may be arranged based on a repeating pattern. For example the openings may be arranged based on a regular lattice such as a square lattice, rectangular lattice, triangular lattice, hexagonal lattice.

Alternatively the openings may be arranged substantially randomly, or offset randomly from a notional regular repeating pattern.

There may be three or more openings. For example there may be 5 or more, 10 or more, 15 or more, 20 or more, 25 or more, 30 or more, 35 or more, 40 or more, 45 or more or 50 or more openings. There are typically fewer than 500 openings, although in some embodiments there may be more openings.

Suitable cross sectional shapes for the openings include circular, oval, elliptical, round, triangular, quadrilateral, rectangular, square, rhombus, pentagonal, hexagonal, pentagonal, octagonal etc. A combination of two or more such shapes may be used for the openings. The openings may have randomly-generated shape. The openings typically have a closed perimeter.

The openings may have a cross sectional area of, for example, at least 0.01 mm^2,at least 0.05 mm^2,at least 0.1 mm^2, at least 0.2 mm^2, at least 0.4 mm^2, at least 0.6 mm^2, at least 0.8 mm^2, at least 1 mm^2, at least 1.5 mm^2, or at least 2 mm^2. There is no particular upper limit on the cross sectional area of the openings, except that a suitable number of openings will need to be fitted to the overall size of the transducer in order to have an effect on the compliance of the relevant component.

The openings may be formed by any suitable manufacturing technique, e.g. machining, cutting (e.g. laser cutting) or etching, or by manufacturing the component with net shape or near net shape techniques such as casting, additive manufacture, etc.

The openings may be filled with a filler material. The filler material may have a Young's modulus that is lower (e.g. a factor of at least 5 lower, at least 10 lower, at least 20 lower or at least 50 lower) than the Young's modulus of the material through with the openings are formed. Suitable materials include epoxy materials or other resin-based materials.

Openings may be formed in two or more of the back mass, front mass and ultrasonic horn arrangement.

The operating frequency of the transducer may for example be at least 1kHz, at least 5kHz, at least 10 kHz, at least 20 kHz, or at least 30 kHz or at least 40 kHz. The operating frequency of the transducer may for example be at most 200 kHz, at most 150 kHz, at most 100 kHz, or at most 90 kHz, at most 80 kHz or at most 70 kHz. For example, a suitable operating frequency is about 55 kHz.

The displacement amplitude at the distal end of the horn may be in the range 1-200 microns peak-to-peak at the operating frequency.

In the method of operation, the ultrasonic transducer may for example be operated at a power in the range 10-1000 Wcm^{-2}.

As mentioned, the openings are formed in one or more of the back mass, front mass and ultrasonic horn arrangement. These are referred to here as the vibrational energy transfer path components of the transducer. Each of said components may have a monolithic construction, i.e. formed from a single piece of material without heterointerfaces (grain boundaries are of course permitted). Accordingly, the requirement that the plurality of openings provide an increased mechanical compliance in a direction along the vibrational energy transfer path for an inventive embodiment arrangement is intended to be compared with a reference arrangement in which the ultrasonic transducer is otherwise identical but in which the openings are replaced with the material of the relevant component. Considering the operating frequency of the transducer of an inventive embodiment arrangement compared with that of a reference arrangement, the operating frequency of the inventive embodiment arrangement may be at least 1 kHz (or at least 2 kHz, or at least 3 kHz, or at least 4 kHz, or at least 5 kHz, or at least 6 kHz, or at least 7 kHz, or at least 8 kHz, or at least 9 kHz, or at least 10 kHz) different (e.g. less) than the operating frequency of the reference arrangement. In turn, this allows inventive embodiment arrangements to have a smaller format than other reference arrangements for the same operating frequency. This means that it is more realistic for such transducers to be located for insertion into the body during surgery, rather than locating the transducers outside the body and using elongate waveguides. In turn, this means that the transducer can be located at the distal side of a flexible joint of a surgical device, allowing more convenient positioning of the transducer.

The length of the transducer (measured from the proximal end of the back mass to the distal end of the horn, along the vibrational energy transfer path) may be not more than 40mm. The maximum diameter of the transducer (measured in a direction perpendicular to the length) may be not more than 15mm.

Still further, considering an inventive embodiment arrangement compared with a reference arrangement as described above, the inventive embodiment arrangement may demonstrate one or more figures of

merit that are the same as or better than the reference arrangement. For example, k_{eff} for the inventive embodiment arrangement may be the same as or better than k_{eff} for the reference arrangement. Additionally or alternatively, Q_m for the inventive embodiment arrangement may be the same as or better than Q_m for the reference arrangement.

The invention includes any combination of the aspects and optional features described except where such a combination is clearly impermissible or expressly avoided.

Summary of the Figures

Embodiments and experiments illustrating the principles of the invention will now be discussed with reference to the accompanying figures in which:

Fig. 1 shows the Harmonic® ACE® + Shears (Ethicon® Endosurgery, Johnson & Johnson, Cincinnati, Ohio, USA).

Fig. 2 shows a generic Da Vinci® end-effector with EndoWrist® technology.

Fig. 3 shows a generic surgical ultrasonic system with its key components.

Fig. 4 shows a schematic perspective cutaway view of a classic d_{33}-mode Langevin-type ultrasonic transducer.

Fig. 5A is a schematic diagram of a symmetric Langevin transducer.

Fig. 5B is a schematic diagram of an asymmetric Langevin transducer.

Figs. 6A and 6B show the effect of the piezoceramic stack length and position in terms of efficiency (Fig. 6A), and normalised figure of merit (Fig. 6B) for high power ultrasonics. The figures are from reference [15].

Fig. 7 shows a schematic view of the serpentine electrodes and how they may be arranged in a piezoelectric stack.

Fig. 8 schematically illustrates the longitudinal vibration mode of a rod, with Poisson's effect.

Fig. 9 shows views of different hollow cylinders used to consider the effect of different holes to modify the apparent Young's modulus.

Fig. 10 shows the shape of holes used for the samples shown in Fig. 9 and the characteristic angle θ.

Figs. 11, 12 and 13 show the longitudinal mode frequency as a function of cylinder length for each hole configuration based on different values for angle θ.

Fig. 14 shows schematic perspective views of BLT models investigated to asses the effect of hole shape and distribution in the front mass.

Figs. 15-18 show the effect that changing the aperture angle has on electrical impedance magnitude and phase of the 4 f.p.p. HC-TSM transducers.

Figs. 19-22 show the effect that changing the aperture angle has on electrical impedance magnitude and phase of the 8 f.p.p. HC-TSM transducers.

Fig. 23 shows a comparison between fitted curves for standard and HC-TSM transducers showing the relationship between L1 f_r and front mass (FM) to back mass (BM) length.

Figs. 24 and 25 respectively show electrical impedance magnitude and electrical impedance phase of standard and HC-TSM 55 kHz tuned transducers.

Figs. 26-30 show views of an exemplary ultrasonic transducer according to an embodiment of the invention. Fig. 26 shows the transducer in front side perspective view. Fig. 27 shows the transducer in rear side perspective view. Fig. 28 shows the transducer in longitudinal cross sectional perspective view. Fig. 29 shows the transducer in exploded side rear side perspective view. Fig. 30 shows the transducer in front perspective view with the horn displaced.

Fig. 31 shows the velocity amplitude with respect to signal frequency of an exemplary ultrasonic transducer.

Fig. 32 shows the displacement amplitude with respect to signal frequency of an exemplary ultrasonic transducer.

Detailed Description of the Invention

Further background to the present invention, and aspects and embodiments of the present invention will now be discussed with reference to the accompanying figures. Further aspects and embodiments will be apparent to those skilled in the art. All documents mentioned in this text are incorporated herein by reference.

A generic surgical ultrasonic system with its key components is shown in Fig. 3. A high-power signal generator 30 is connected to the power source 32 and controls an ultrasonic transducer, indicated

generally by reference number 34. The ultrasonic transducer is a key element of the system, as it converts electrical energy into useful mechanical vibration. A typical operating frequency of the transducer is in the range 20-100 kHz for surgical applications. The ultrasonic transducer is normally located within a casing 36 so it can be handled safely. On one end of the transducer, a probe (waveguide) 38 is attached to guide the wave towards the tissue. As shown schematically in Fig. 3, the transducer includes a piezoelectric stack 40 sandwiched between a front mass 42 and a back mass 44. A horn 46 is located between the front mass 42 and the waveguide 38.

Each of the system's components has its own role and importance, and the design of each part follows certain rules to achieve the desired frequency, performance, and effect in tissue.

The design guidelines for Langevin transducers are the result of many years of successful applications. Numerous books, papers and theses have reported extensively on them. See for example Refs 8, 9 and 10. A brief overview of significant design specifications is given below, as a guide for design considerations.

The schematic perspective cutaway view of a classic d_{33}-mode Langevin-type ultrasonic transducer shown in Fig. 4 uses similar reference numbers to Fig. 3 for corresponding features.

The ultrasonic transducer is, in many known devices, inspired by the sandwich configuration introduced by Langevin and Chilowsky, firstly applied in underwater sound projectors in 1918 [1]. The Langevin design, also called 'Tonpilz', from the German for 'singing mushroom', simply consists of a stack of piezoelectric rings (normally piezoceramic), with intervening electrodes 52, the stack prestressed between a back mass 44 and a front mass 46 with a prestressing bolt 50 [8]. These types of transducers are also known as bolted Langevin transducers (BLTs). In Fig. 4, the front mass includes a flange 54 at the rear end of the front mass and cooling holes 56 formed through the flange 54.

As a starting point for design, the case of a thin rod, where the diameter d is considerably smaller than the length l ($d << l$), may be compared to a Langevin transducer to introduce some fundamental concepts. With the assumption of the thin rod, the approximate length of the transducer is half of the wavelength, λ, defined in Equation 1,

$\lambda = \frac{c}{f}$	Equation (1)

where c is the speed of sound in the rod and f the desired operational frequency. The speed of sound in a specific material is defined in Equation 2,

$c = \sqrt{\frac{E_M}{\rho}}$	Equation (2)

where E_M is the Young's modulus, and ρ the material's density. Equation 3 shows how the natural frequencies, f_n, for the longitudinal vibrational modes n (n = 1,2,3...) of a thin rod, can be estimated.

$f_n = \frac{n}{2\,l} c$	Equation (3)

Fig. 5A is a schematic diagram of a symmetric Langevin transducer. If the transducer can be divided centrally at the nodal plane, each half of the transducer, corresponding to $\frac{\lambda}{4}$ in length can be studied independently.

Fig. 5B is a schematic diagram of an asymmetric Langevin transducer.

The relationship between the resonant frequency (recalling that $\omega = 2\pi f$), the acoustic impedance, ζ, and the length of both the piezoelectric stack and end masses is expressed by Equation 4.

$\frac{\zeta_m}{\zeta_p} tan\left(\frac{\omega_p l_p}{v_p}\right) tan\left(\frac{\omega_m l_m}{v_m}\right) = 1$	Equation (4)

The subscripts *p* and *m* represent piezoelectric and end-mass (either the back or the front mass) respectively. l_p and l_m are the thickness of the piezoelectric ring and the length of the end-mass, respectively. ζ_m is the acoustic impedance of an end-mass, which can be obtained from Equation 5:

$\zeta_m = \rho_m c_m A_m$	Equation (5)

and ζ_p is the acoustic impedance of the piezoelectric element obtained from Equation 6:

$\zeta_p = \rho_p c_p A_p$	Equation (6)

where *A* is the cross-sectional area of the component.

Equation 4 can be used to approximate the resonant frequency of a transducer with known dimensions or to find an unknown dimension if the frequency and other parameters are known [12].

The piezoelectric stack 40 is generally made with either d_{33}-mode rings or a d_{31}-mode ring. In high power applications, 'hard' piezoceramic such as PZT 4 and PZT 8 is used in even numbers of rings to create the piezoelectric stack, placed between the front and back masses with electrodes in between.

The total length of the piezoelectric stack is chosen to be approximately one quarter of *l*. However, the choice is influenced by the available driving electronics, as increasing ceramic thickness needs a higher driving electric field and has higher electrical impedance, higher mechanical losses and higher capacitance, resulting in overall higher costs [13].

The centre of the stack is best located at the nodal plane, labelled 'node' in Fig. 5A, located in the centre of the transducer in a symmetric design, where the strain is highest. The stack position affects both resonant frequency and vibration amplitude, therefore its location is an important aspect of the design process [14].

Commonly, to allow placement of a supporting flange to attach a casing, the piezoelectric stack is placed away from the nodal position towards the back mass, as shown in Fig. 5B, in an asymmetric

configuration. In this configuration, the flange has minimal impact on the vibrational mode. In the asymmetric design, each $\frac{\lambda}{4}$ section can be analysed independently and if the half of the transducer including the back mass, the piezoceramic stack, and part of the front mass, *l1*, is considered, Equation 7 can be used to estimate either the frequency or an unknown dimension of the transducer.

$\frac{\zeta_m}{\zeta_p}\tan\left(\frac{\omega_p l_p}{v_p}\right)\tan\left(\frac{\omega_m l_m}{v_m}\right)+\frac{\zeta_m}{\zeta_{l1}}\tan\left(\frac{\omega_{l1} l_1}{v_{l1}}\right)\tan\left(\frac{\omega_m l_m}{v_m}\right)+\frac{\zeta_p}{\zeta_{l1}}\tan\left(\frac{\omega_{l1} l_1}{v_{l1}}\right)\tan\left(\frac{\omega_p l_p}{v_p}\right)=1$	Equation (7)

It has been shown by Lierke [15] that the maximum efficiency of the transducer is achieved when the piezoceramic stack is centred and its length is half of the total length of the transducer. The greater the offset from the node, the lower the efficiency, k_{eff}^2, as shown in Fig. 6A. When considering the figure of merit, normalised by the maximum of $k_{eff}^2 Q_m$, again the best position for the piezoelectric stack is found to be in the centre of the transducer. The normalised figure of merit is above 90% when the ratio $L_{piezo}/L_{transducer}$ is between 0.2 and 0.5, as shown in Fig. 6B [15].

The electrodes are normally chosen with material properties (density, elastic modulus, and acoustic impedance) similar to the piezoelectric materials to avoid unwanted stress concentrations. Note that here we refer to “electrodes” as separate entities from any metallisation formed on the piezoelectric materials.

In hand-held transducers, serpentine electrodes 52a, 52b, shown in Fig. 7, may be used in order to provide electrical contact to each side of the respective piezoelectric rings 58. Each piezoelectric ring takes the form of an apertured disk, with the aperture 60 formed through the disk 58 along its principal axis. The left hand part of Fig. 7 shows one electrode 52a and one piezoelectric ring 58 separately. The right hand part of Fig. 7 shows two serpentine electrodes 52a, 52b and four piezoelectric rings R_1, R_2, R_3, R_4 forming the piezoelectric stack. Each serpentine electrode 52a, 52b has electrode ring portions spaced and disposed in order to be located against end faces of respective piezoelectric rings and connecting portions between the electrode ring portions. Such serpentine electrodes are useful in that they can have only limited lateral protrusion and few terminating wires, and no soldering is needed in the vicinity of the rings. The only required soldering is carried out at soldering areas 62, indicated. Cooling fins can also be found in some applications [16].

Metallization on the piezoelectric elements (rings) is normally prepared with 3-10 µm layers obtained through sputtered depositions, electroplating, or special coatings of Cr, Ni, or Au, or other combinations depending on the material suppliers, and these form the interface between the piezoelectric elements and the electrodes.

A prestressing bolt is used to apply and distribute the prestress within the stack. Titanium is the preferred material due to its high strength and capability to withstand cyclic loads. The primary reason for prestress is to prevent the piezoceramic from experiencing excessive tensile stress during vibration as

piezoceramics are typically almost seven times weaker in tension than in compression. Moreover, the prestress helps to stabilise both the resonance frequency and impedance magnitude and, in addition, it ensures continuity of electrical contact during high level of vibrations [16].

The fundamental desired characteristics of a prestressing bolt are low stiffness, achieved with long bolts, small shank diameter, and low Young's modulus, and high resistance to cyclic loads. The threads of the bolt stretch when the front mass stretches, and the generated friction between the bolt and the front mass can cause undesired heating and subsequent failure (e.g. via fatigue failure) of the thread. The stiffness of a prestressing bolt may be equal to or lower than the front mass stiffness, and may be lower than the piezoceramic stack stiffness. However, long transmission bolts suffer more from mechanical failure [17].

Generally, the required and optimal prestress to apply is not specified and it changes with each design and with the piezoelectric material used. The typical prestresses applied to hard piezoceramics are in the range 25-50 MPa for PZT 4 and 30-79 MPa for PZT 8 [16]. It is important to note that piezoceramic performance degrades with increasing prestress, which causes reductions in piezoelectric coefficients and maximum operating temperature; it may also cause piezoelectric material depolarisation and increase mechanical losses. All these parameters are also known to deteriorate more over time when prestress is applied.

Regarding piezocrystal behaviour under prestress conditions, it has been reported (see references [18] to [20]) that uniaxial pressure, in the range of 0-60 MPa, negatively affects electromechanical properties, with the same consequences as highlighted for piezoceramics. Additionally, piezocrystals may also experience phase transitions under the simultaneous combination of high-power electric field and uniaxial pressure [21].

The back mass has a principal role as an inertial mass, and it also distributes the prestress laterally across the piezoceramic rings. It is normally a solid cylinder, but it has been reported that conic shapes can be used, increasing the bandwidth of the transducer [22]. A rule of thumb for a back mass made of steel indicates that its length should be at least 45% of the diameter of the piezoceramic stack, and its diameter should be at least equal to that of the piezoceramic stack. If other materials are used instead of steel, then the Young's modulus may be used as a comparison, and dimensions adjusted accordingly, in inverse proportion. For example, if a material with half the Young's modulus of steel is used, then the length of the back mass should be doubled (see references [8] to [10] and [23]).

The front mass transfers the vibrational energy to the horn and the probe/blade and often includes a flange which connects to the case. The flange sometimes includes holes for air cooling. Sometimes it can be combined with the horn and they can be machined together as it is often made of the same material but, when this is not possible, either spanner holes or wrench flats are provided to connect the front mass and horn with a thread. In surgical tools, wrench flats are preferred as more suitable for small

diameter devices. The material used in the front mass is typically more compliant and less dense compared to the material used for the back mass, to facilitate the transfer of the ultrasonic vibration [24].

The horn is a mechanical amplifier which increases the vibration amplitude from the front mass: the vibrational energy travelling through a constant cross-sectional area remains constant; but if the cross-sectional area is progressively reduced along the direction in which the vibrational energy is travelling, then the vibrational energy density and the amplitude increase.

Different horn designs can be used such as stepped, linear or tapered, and exponential, as will be understood by the skilled person. Some horns convert the vibration from the longitudinal mode into a torsional or a transversal mode by using incisions on the surface. In some cases, multiple horns are linked together in cascade, with the amplification sections called 'boosters' [24] [25].

The case protects the user from the high voltage and current needed for transducer excitation and also from excess heating. It is designed to clamp the device at its nodal plane so that the fundamental vibrational mode of the device will not be affected.

The waveguide or probe is generally a rod like structure which guides the wave to the tip-end. In devices for soft tissue cutting used in laparoscopic surgery, the tip-end is normally a blade at the end of a long wave guide. It is normally made of Ti6Al4V alloy (90% titanium, 6% aluminium, 4% vanadium, 0.25% iron and 0.2% oxygen) in order to handle the cyclic stresses of the ultrasonic vibrations and at the same time to ensure that it can withstand any loading. The length of the transmission rod is an integer number of half wavelengths, at the operational resonance frequency of the device, and it attaches to the horn at an antinode [26].

The blade at the end of the probe transfers the ultrasonic energy to the tissue and it is shaped according to the desired effect/application. Various blade designs are outlines below.

Suitable blade tips:

(a) for soft-tissue cutting and sealing: THUNDERBEAT® type S, Olympus® Medical [3];
(b) for ultrasonic aspiration: SONOPET® (Stryker®, Kalamazoo, MI, USA);
(c) for precise cutting of bone for reuse elsewhere in the body: SONOPET® Payner® 360 bone tip, (Stryker® [27]) [28];
(d) for bone cutting: SONOPET® bent blade (Stryker®) [29].

As already indicated, an important aspect of the transducer design process is the choice of the materials to be used, which depends on their properties and application requirements.

The Young's modulus, E_M, quantifies the stiffness of elastic materials, defined in Equation 8:

$E_M = \frac{\sigma}{\epsilon} = \frac{\frac{F}{A}}{\frac{dl}{l}} = \frac{Fl}{Adl}$	Equation (8)

as the ratio between stress σ and strain ε, where *F* is the force applied to the material through a cross sectional area *A*, and *dl* is the change of length and the initial length is *l*, along an axis.

The elasticity indicates how a material restores to its original shape after distortion, and the restoring force is proportional to the stress applied. The elasticity is described by Hooke's Law, Equation 9:

$F = k\, dl$	Equation (10)

where *k* represents the stiffness.

As is widely understood, Hooke's Law is valid only in the elastic region of the stress-strain curve, which is the part of the curve up to the yield strength. A general material may undergo:

- *tensile stress* when normally stretched.
- *compressive stress* when normally compressed.
- *shearing stress* when sheared in plane to the stressed area.

Another important parameter in the choice of materials is the acoustic attenuation. When longitudinal sound waves propagate through a medium, their intensity reduces from the source. Energy loss phenomena are due to scattering and absorption, which are caused by motion of the wave in other directions than the longitudinal and heat generation due to friction. Materials with low acoustic attenuation are preferred; these include light alloys made with metals such as titanium, aluminium and magnesium; heavier material such as brass and tungsten should be avoided if possible. A simple way to look at this is via the longitudinal sound velocity: the faster the speed of sound in a material, the less the energy loss [10].

During cyclic tensile loading, a transducer's components will dynamically deform, experiencing high levels of both stress and strain, dependent on both material properties and the shape of the component, e.g., with sharp corners and step profiles. These forces can concentrate, causing heating and failure e.g., through cracking. A typical design guide indicates that the ultimate tensile strength of each material should be 30% higher than the maximum stress experienced by the tool in operational conditions [30].

Transducer components should also be acoustically matched. The speed of sound in a material is dependent on E_m and ρ (Equation 2), but when another material is present, some of the energy will be transmitted forward and some will be reflected back from the interface between the materials, with the possibility that some energy will be converted into a different wave mode.

The amount of energy reflected back is expressed with the reflection coefficient, R_c, in Equation 10:

$R_c = \frac{\zeta_2 - \zeta_1}{\zeta_2 + \zeta_1}$	Equation (10)

where ζ_1 and ζ_2 are the acoustic impedance of the first and second media respectively.

The closer the acoustic impedance of the materials, the more energy will be transmitted through the interface, which is desirable for efficient devices. Back and front masses should be made with different materials, with the 'lower density' one used for the front mass. This contributes to a larger vibrational amplitude at the front of the transducer. Hence, Equation 11:

$\zeta_{piezo} = \sqrt{\zeta_{front\ mass}\, \zeta_{back\ mass}}$	Equation (11)

should be respected to achieve maximum energy transmission between the piezoelectric stack and the front mass [10], [31].

Ultrasonic energy can be applied to media to generate different vibrational modes, the simplest of which is the longitudinal mode shown in Fig. 8, where consecutive expansions and contractions along the transducer longitudinal axis are observed with lateral motion simultaneously observed, caused by Poisson's ratio [24].

The longitudinal mode may also be used to generate other modes by modifying the waveguide and/or the horn as noted previously. Asymmetric longitudinal motion can be achieved by using asymmetric blades to add lateral vibrations to the longitudinal motion, making the cutting procedure more effective in certain applications, as previously mentioned for ultrasonic bone-cutting surgical tools.

The cutting mechanisms and dynamics of action depend on the specific surgical task. Cavitation is used in tissue-preserving devices, the direct impact or 'jackhammer effect' in bone cutting devices, and the thermal effect is adopted in devices for soft tissue cutting and coagulation.

In ultrasonic cutting devices used in soft tissue, the thermal effect is desired, and the tissue is heated to the point of denaturation. The tip of a device to generate this effect has a decoupled bifurcation, as shown in the inset of Fig. 1, allowing the jaw to move and force the tissue onto the ultrasonic vibrating blade. The clamping pressure necessary to close the jaw is applied by the surgeon's hand through a mechanical lever. The induced friction causes the tissue to be heated, denaturated and cut in within few seconds, with no bleeding.

The interaction between soft tissue and ultrasonic devices is complex, depending on the protein and water content of the tissue undergoing the surgical procedure. In general, tissue with high water content is easier to cut, whereas tissue with high protein content, such as blood vessels, nerves and connective

tissue, requires more energy. The temperature can exceed 100 °C which is sufficient to denature proteins and, if the tissue is heated above its critical necrotic temperature, the damage is irreversible and beyond repair.

The cutting and haemostatic effects are not independent and they happen simultaneously. However, one can be predominant depending on the frequency and vibration amplitude of the blade. Lower frequency and higher vibration result in faster cutting and slower coagulation, while higher frequency and lower vibration cause slower cutting and faster coagulation [25], [26].

The Da Vinci® Surgical System (Intuitive® Surgical, Inc.) was introduced along with the EndoWrist® above. The Harmonic® ACE + Shears (Ethicon® Endo-Surgery) is to date the only Da Vinci®-compatible ultrasonic surgical tool. One of the drawbacks of this tool is its lack of manoeuvrability, i.e. incompatibility with the EndoWrist® technology. This incompatibility is due to several interrelated reasons which are discussed below.

First we consider the operational frequency and device configuration. Ultrasonic surgical devices with haemostatic dissection capability generally operate at about 55 kHz [34]. The operational frequency of a BLT is linked to the device length. Generally, BLTs are designed to operate primarily at their first longitudinal vibrational mode, L1, corresponding to half-wavelength. This puts a constraint on the device length. Additionally, the piezoelectric stack volume and position affect the device's efficiency and functionality. This determines the number of piezoelectric ring elements and their diameter within the stack to achieve the required vibrational amplitude performance. Under these conditions, the device cannot be miniaturised without compromising its operational frequency and without degrading performance, i.e. blade longitudinal vibration amplitude (about 80 μm) [35].

Next we consider the waveguide. From the previous conditions, it emerges that the resulting ultrasonic transducer is effectively too long and large to fit into a laparoscopic port; therefore, a waveguide is used to transfer the vibration from the transducer outside the human body to the end effector (blade) inside the human body. Consequently, this design limits the manoeuvrability of the blade in view of the need for the waveguide to be long enough to allow the transducer to be outside the body. In order to improve the manoeuvrability of the blade, it would be useful to include a wristed joint integrated at the end effector of the device. However, this would present an interruption in the waveguide and therefore an interface including a discontinuity. In that case, the ultrasonic wave would not be transmitted towards the blade but would be reflected, resulting in a non-moving blade.

The present inventors have considered whether any previous developments in this field would be useful to assist in the miniaturisation of an ultrasonic transducer that would be useful for surgery.

For example, in [36], BLT optimisation was carried out to miniaturise an ultrasonic scalpel for vessel cutting and sealing and integrate the device with a multi-degree of freedom end-effector for the Micro Hand® S robotic system (Tianjin University, China). A 55 kHz resonating device approximately 50 mm in length, and 10 mm in diameter was developed. The device was successfully integrated and mounted beyond a wrist-like joint and blade displacement of more than 100 µm was reported. Ex vivo experiments were carried out on chicken tissue, demonstrating the functionality and the potential of the device. Effectively, however, the work reported does not present any innovative miniaturisation strategy; since the length of the fabricated device is approximately what is expected for a 55 kHz resonator and is too large for practical laparoscopic surgery.

[37] and [38] report a folded horn transducer, in which the design of the horn allowed a reduction of the horn length by a factor of two whilst maintaining the same operational frequency. While this design reduces the overall length of the device, it does not decouple from the actual horn length.

Flextensional transducers are assembled with a piezoelectric disc sandwiched between two cymbal-shaped metal end caps. Several improvements have been reported for this design, such as the introduction of bolts to prevent failure due to the bonding epoxy layers because of high-power driving. Flextensional transducers can have a relatively small format. However a disadvantage of this design is the possible asymmetry arising from the epoxy bonding layers, which may alter the vibrational mode of the device. Moreover, typical designs exploits the radial mode of a piezoelectric disc, which is not suitable for anisotropic piezocrystals.

A planar ultrasonic silicon scalpel was reported in [42] and [43]. This design used PZT piezoceramics and it was able to achieve a blade vibrational amplitude of about 50 µm at 68 kHz. The device dimensions were length = 80 mm, thickness = 20 mm and width = 22.5 mm, which makes it unsuitable for miniaturisation with the present configuration and material properties of Si. This design was also shown and demonstrated with piezocrystals [23].

Another use of the d_{31} mode demonstrated the use of piezocrystals for the actuation of a standard needle for anaesthesia [44]. The design incorporated back and front masses and, for this reason, it can be termed a pseudo-Langevin device for its similarity with the piezoelectric ring stack configuration. This design achieves a needle tip displacement of less than 10 µm at 70 VPP. Moreover, the operating frequency of the device is approximately 80 kHz, and the total length without the needle is more than 40 mm. This means that to achieve 55 kHz the device total length must be increased, making this design even less suitable for miniaturisation purposes. A further drawback of these designs is the presence of a bonding layer, in this case made of conductive epoxy, which could fail under high vibrational stresses. Another bonding-related issue with this design can be attributed to the corrupted vibrational mode symmetry which causes stress concentration points which may cause device failure at high vibrational stresses, i.e. detachment from the substrate and cracking.

Next we consider the needs of robotic surgery, relevant to the present disclosure. The superior dissection quality and the speed of sealing of ultrasonic devices, over standard electrocautery, is reported in many studies, e.g. [45]. It is interesting to note that, only a few studies mention the generation of surgical smoke during the procedure [46], [47]. This may reduce laparoscopic visibility and cause delay in the overall procedure time due to endoscope cleaning.

In robotic surgery, ultrasonic dissectors are used predominantly in parenchymal transections to separate the functional tissue of an organ from the connective and supporting tissue, and in lobectomies to remove a lobe or a portion of an organ [5], [6], [48]. Popular robotic procedures, involving the use of ultrasonic dissectors to perform specific intra-operative tasks, include: hepatectomies, splenectomies, enterectomies, adrenalectomies, and thyroidectomies. A study on robot-assisted thyroid surgery [49] compared a wristed bipolar electrocautery instrument (Vessel Sealer Extend, Intuitive® Surgical, Inc.) with an ultrasonic dissector (Harmonic® ACE + Shears, Ethicon® Endo-Surgery).

The direct comparison showed that the use of the ultrasonic device reduced the intra-operative blood loss and improved the dissection margins and speed of seal when compared with the standard electrocautery instrument. However, a higher risk of patient injuries such as burns and involuntary tissue perforations was found with the ultrasonic device, due to the combination of the high temperature of the waveguide and the lack of instrument manoeuvrability. Therefore, an ultrasonic dissector with a flexible joint, mounted at the end of the robotic shaft beyond the wrist, would address these issues.

The present invention is based on the realisation that it is possible to engineer the stiffness of components of an ultrasonic transducer in order to address some of the design constraints identified above and to decouple f_r for the longitudinal mode from the device length. The word “metastructure” is used in the present disclosure (similarly to the concept of a “metamaterial”), indicates a structure engineered to exhibit mechanical properties which differ from those of the bulk material from which the structure is made.

Equation 3 showed the relationship between the natural frequency of the longitudinal mode, the speed of sound and the length of a thin rod. Considering n = 1, and replacing *c* with its mathematical definition (Equation 2), Equation 12 is obtained:

$f_n = \frac{1}{2l}\sqrt{\frac{E_M}{\rho}}$	Equation (12)

Young’s modulus represents the stiffness of a material, therefore rod-like structures made with materials with low E_M will vibrate longitudinally at lower frequencies than less compliant (more stiff) materials. Thus, in the context of embodiments of the present invention, it is of interest to change (or tune) the stiffness of a rod-like structure to make it resonate at a desired frequency without altering its length?

A review of mechanical metamaterials [50] shows some strategies to change the mechanical properties of a structure by engineering the unit cells forming the overall lattice. In particular, it is possible to alter the apparent Young's modulus of a structure in one or more directions, typically leading to an increase in anisotropy of the Young's modulus for the structure.

To implement this concept for ultrasonic transducers, a study was performed and results successfully indicated that a transducer cylindrical component can be engineered to modify its apparent Young's modulus and therefore modify the frequency of the longitudinal mode without altering the transducer length. In this study, three different formats for a hollow cylindrical component were considered, each being suitable for use as a front mass of a BLT transducer.

As shown in Fig. 9, the Hexagonal sample used an array of hexagonal through-holes through the wall of the hollow cylinder, with a total number of holes being 54. The arrangement of the holes was based on a hexagonal lattice. Considering the centre of each hole, these centres were arranged so that the centres were each aligned with a plane perpendicular to the principal axis of the cylinder, there being 6 centres per plane, regularly circumferentially spaced around the cylinder. In the drawing, the axial length of the cylinder was 12 mm but this is for illustration only – in the modelling, the axial length of the cylinder was changed in order to show the effect on stiffness of the arrangement of the holes. The force F was applied along the principal axis of the cylinder.

The SpringNet sample shown in Fig. 9 was identical to the Hexagonal sample except for the shape of the holes, which were rhombus shape.

The Holes sample shown in Fig. 9 was identical to the Hexagonal sample except for the shape of the holes, which were oval shape.

The shape of holes for each sample was changed based on Fig. 10. For each hole, angle θ is defined, based on a height of the hole being 1.5 mm measured in a direction parallel to the principal axis of the cylinder.

Figs. 11, 12 and 13 show the longitudinal mode frequency as a function of cylinder length for each hole configuration based on different values for angle θ.

For a non-hollow cylinder, E = 121 GPa (i.e. the Young's modulus of the bulk material) and the frequency response is shown by the upper dashed line. For a hollow cylinder, the apparent Young's modulus is 42 GPa and the frequency response is shown by the lower dashed line. Each sample incorporating holes arranged as described has a lower resonant frequency for a particular length of cylinder compared with the hollow cylinder. Or, put another way, adding holes reduces the length of the cylinder needed in order

to achieve a particular resonant frequency. Furthermore, decreasing angle θ for each type of hole leads to a reduction in resonant frequency.

Based on the study reported above, further investigations were carried out based on the honeycomb (HC) shaped holes. This choice was made because the HC showed great capability in lowering the resonant frequency without introducing other vibrational modes in proximity to L1. The abbreviation TSM used herein refers to Tuneable Stiffness Metastructure.

HC-TSM angle θ and the number of HC-TSM features per plane (f.p.p.), were investigated under the hypothesis that these variables should have an impact on the apparent Young's modulus, hence on f_r for the L1 mode. All the models investigated in this study are shown in Fig. 14. The results of the design study on HC-TSM are presented and discussed for the L1 mode only, as it represents the vibrational mode of interest for ultrasonic transducers for surgical applications.

Figs. 15-18 show the effect that changing the aperture angle has on electrical impedance magnitude and phase of the 4 f.p.p. HC-TSM transducers. Figs. 19-22 show the effect that changing the aperture angle has on electrical impedance magnitude and phase of the 8 f.p.p. HC-TSM transducers.

Figs. 15 and 17 show that in the broader spectrum, 0-300 kHz, changes can be observed in electrical impedance magnitude and phase, and the frequency location of the L1 mode. Figs. 16 and 18 show the data in the vicinity of the L1 mode. These show that the L1 mode was found to drop in frequency as a consequence of reducing the aperture angle from 120° to 90° and to 60°. The electrical impedance magnitude and phase of the standard transducer are also included for reference.

Similarly, Figs. 19 and 21 show that in the broader spectrum, 0-300 kHz, changes can be observed in electrical impedance magnitude and phase, and the frequency location of the L1 mode. Figs. 20 and 22 show the date in the vicinity of the L1 mode. These show that the L1 mode was found to drop in frequency as a consequence of reducing the aperture angle from 120° to 90° and to 60°. The electrical impedance magnitude and phase of the standard transducer are also included for reference.

Table 2 shows the effect of the introduction of HC-TSM on the relevant transducer parameters of the L1 mode. The key point that emerges from this design study is that the L1 mode was altered without modifying the length of the transducer. In addition, minor but positive changes were observed in other transducer properties, such as reduced electrical impedance magnitude at f_r and improved operational bandwidth.

Table 2: Results summary from the L1 mode for the studied design variables in the HC-TSM transducer.

	f_r	Z@ f_r	f_a	Z@ f_a	k_{eff}	Q_m
FEA Model	kHz	kΩ	kHz	kΩ	/	/

Standard	*f.p.p.*	*angle*	74.99	0.32	76.92	4.11	0.22	65.88
		120°	71.25	0.36	73.11	4.68	0.22	65.10
HC-TSM	4	90°	69.97	0.36	71.83	4.92	0.22	66.13
		60°	67.27	0.35	69.17	5.49	0.23	68.29
		120°	66.65	0.32	68.69	6.11	0.24	70.26
HC-TSM	8	90°	64.64	0.30	66.72	6.70	0.24	70.88
		60°	57.67	0.28	59.90	9.28	0.27	75.28

It is therefore possible to make a comparison between a "standard" 55 kHz transducer and an exemplary HC-TSM transducer, where the transducers differ in the construction of the front mass based on the discussion set out above. The most important initial comparison that can be made between the two transducer models is the capability of the HC-TSM device to resonate at the L1 mode with a lower frequency than the standard device despite being of equal length and made from the same materials, as shown in Fig. 23.

Figs. 24 and 25 respectively show electrical impedance magnitude and electrical impedance phase of standard and HC-TSM 55 kHz tuned transducers. The electrical impedance magnitude and phase spectra in Figs. 24 and 25 show that the curve fitting was able to correctly determine the length of FM-BM for a 55 kHz resonating device in both cases.

Table 3 compares the device parameters for the L1 mode of the devices. The introduction of HC-TSM enabled a transducer design which was 20.5% shorter in length than the standard design with approximately the same f_r. Moreover, the HC-TSM transducer presents 30% lower electrical impedance at resonance and 28% more bandwidth than the standard design.

Table 3: Extrapolated device parameters from simulated electrical impedance of Figs 24 and 25 for 55 kHz-tuned devices for the L1 mode.

	Tot. Length	f_r	**Z@** f_r	f_a	**Z@** f_a	k_{eff}	Q_m
FEA Model	mm	kHz	kΩ	kHz	kΩ	/	/
Standard	44.00	55.20	421.16	56.43	5.87	0.21	78.81
8 *f.p.p, angle* 60°, HC-TSM	35.00	55.08	294.33	57.13	9.78	0.27	75.50

Figs. 26-30 show views of an exemplary ultrasonic transducer according to an embodiment of the invention. Fig. 26 shows the transducer in front side perspective view. Fig. 27 shows the transducer in rear side perspective view. Fig. 28 shows the transducer in longitudinal cross sectional perspective view. Fig. 29 shows the transducer in exploded side rear side perspective view. Fig. 30 shows the transducer in front perspective view with the horn displaced.

In each of Figs. 26-30, the transducer has a back mass 44 and a front mass 46 with horn 48 located forwards of the front mass. Two piezoceramic rings 58 of opposing polarity sandwich an electrode 52 to form a piezoelectric stack (ultrasonic actuator arrangement) which is held between the back bass and the front mass by prestressing bolt 50 and nut 51. The front mass has an outer cylindrical wall with an arrangement of holes (in this case circular holes) formed through it. In operation, a driving signal is applied to electrode 52 and the front and back masses are earthed, causing oscillation of the piezoelectric rings.

The achievable vibrational amplitudes of standard and HC-TSM 55 kHz transducers were compared. The HC-TSM transducer showed a 33% higher displacement at the blade tip than the standard design for the same driving signal.

Fig. 31 shows the velocity amplitude with respect to signal frequency of the exemplary ultrasonic transducer. Note that although the legend indicates a signal with V_{rms} of 0.8 V, there are no data points for this. Instead, the lowest curve is for V_{rms} of 3.5 V and the curves progressively increase up to V_{rms} of 73 V.

Fig. 32 shows the displacement amplitude with respect to signal frequency of the exemplary ultrasonic transducer. The lowest curve is for V_{rms} of 0.8 V and the curves progressively increase up to V_{rms} of 73 V.

***

The features disclosed in the foregoing description, or in the following claims, or in the accompanying drawings, expressed in their specific forms or in terms of a means for performing the disclosed function, or a method or process for obtaining the disclosed results, as appropriate, may, separately, or in any combination of such features, be utilised for realising the invention in diverse forms thereof.

While the invention has been described in conjunction with the exemplary embodiments described above, many equivalent modifications and variations will be apparent to those skilled in the art when given this disclosure. Accordingly, the exemplary embodiments of the invention set forth above are considered to be illustrative and not limiting. Various changes to the described embodiments may be made without departing from the spirit and scope of the invention.

For the avoidance of any doubt, any theoretical explanations provided herein are provided for the purposes of improving the understanding of a reader. The inventors do not wish to be bound by any of these theoretical explanations.

Any section headings used herein are for organizational purposes only and are not to be construed as limiting the subject matter described.

Throughout this specification, including the claims which follow, unless the context requires otherwise, the word “comprise” and “include”, and variations such as “comprises”, “comprising”, and “including” will be understood to imply the inclusion of a stated integer or step or group of integers or steps but not the exclusion of any other integer or step or group of integers or steps.

It must be noted that, as used in the specification and the appended claims, the singular forms “a,” “an,” and “the” include plural referents unless the context clearly dictates otherwise. Ranges may be expressed herein as from “about” one particular value, and/or to “about” another particular value. When such a range is expressed, another embodiment includes from the one particular value and/or to the other particular value. Similarly, when values are expressed as approximations, by the use of the antecedent “about,” it will be understood that the particular value forms another embodiment. The term “about” in relation to a numerical value is optional and means for example +/- 10%.

References

A number of publications are cited above in order to more fully describe and disclose the invention and the state of the art to which the invention pertains. Full citations for these references are provided below. The entirety of each of these references is incorporated herein.

[1] D. Zimmerman, “‘A more creditable way’: The discovery of active sonar, the Langevin–Chilowsky patent dispute and the Royal Commission on Awards to Inventors,” War Hist., vol. 25, no. 1, pp. 48–68, 2018, doi: 10.1177/0968344516651308.

[2] S. K. Longmore, G. Naik, and G. D. Gargiulo, “Laparoscopic Robotic Surgery : Current Perspective and Future Directions,” 2020, doi: 10.3390/robotics9020042.

[3] Olympus, “Thunderbeat,” 2020. https://www.olympus-global.com/technology/technology/thunderbeat/?page=technology_technology (accessed Apr. 28, 2020).

[4] “Ethicon Harmonic Ace.” https://www.ethicon.com/na/epc/code/harh36?lang=en-default.

[5] M. Kroh, Essentials of Robotic Surgery. Springer, 2015.

[6] G. Spinoglio, Robotic Surgery Current Applications and New Trends. Springer, 2015.

[7] S. L. Best and S. Y. Nakada, Minimally Invasive Urology. Springer, 2015.

[8] C. H. Sherman and J. L. Butler, Transducers and Arrays for Underwater Sound. 2013.

[9] D. Stansfield and A. Elliott, Underwater Electroacoustic Transducers: Second Edition. Peninsula Publishing, 2017.

[10] A. Mathieson, “NONLINEAR CHARACTERISATION OF POWER ULTRASONIC DEVICES USED IN BONE SURGERY,” University of Glasgow, 2012.

[11] U. Resonators, “Piezoelectric transducer design,” 2020. http://www.ultrasonic-resonators.org/design/transducers/transducer_design.html#mode_33 (accessed Apr. 26, 2020).

[12] E. A. Neppiras, “The prestressed piezoelectric sandwich transducer,” Ultrason. Int., 1973.

[13] D. A. Deangelis and G. W. Schulze, “Optimizing Piezoelectric Ceramic Thickness in Ultrasonic Transducers,” Proc. 39th Annu. Symp. Ultrason. Ind. Assoc., pp. 1–9, 2010, doi: 10.1109/UIA.2010.5506062.

[14] A. Mathieson, A. Cardoni, N. Cerisola, and M. Lucas, “The Influence of Piezoceramic Stack Location on Nonlinear Behavior of Langevin Transducers,” vol. 60, no. 6, pp. 1126–1133, 2013.

[15] E. G. Lierke, W. Littmann, T. Morita, and T. Hemsel, “Various Aspects of the Placement of a Piezoelectric Material in Composite Actuators , Motors , and Transducers,” vol. 57, no. 4, pp. 933–937, 2010, doi: 10.3938/jkps.57.933.

[16] D. A. Deangelis and G. W. Schulze, “Optimizing Piezoelectric Crystal Preload in Ultrasonic Transducers,” 2009 38th Annu. Symp. Ultrason. Ind. Assoc., pp. 1–6, doi: 10.1109/UIA.2009.5404031.

[17] D. A. Deangelis, G. W. Schulze, and K. S. Wong, “Optimizing piezoelectric stack preload bolts in ultrasonic transducers,” Phys. Procedia, vol. 63, pp. 11–20, 2015, doi: 10.1016/j.phpro.2015.03.003.

[18] X. Liao et al., “Functional piezocrystal characterisation under varying conditions,” Materials (Basel)., vol. 8, no. 12, pp. 8304–8326, 2015, doi: 10.3390/ma8125456.

[19] D. Viehland, “Effect of Uniaxial Stress Upon the Electromechanical Properties of Various Piezoelectric Ceramics and Single Crystals,” J. Am. Ceram. Soc., vol. 89, no. 3, pp. 775–785, 2006, doi: 10.1111/j.1551-2916.2005.00879.x.

[20] Z. Qiu et al., “Characterization of piezocrystals for practical configurations with temperature- and pressure-dependent electrical impedance spectroscopy.,” IEEE Trans. Ultrason. Ferroelectr. Freq. Control, vol. 58, no. 9, pp. 1793–803, 2011, doi: 10.1109/TUFFC.2011.2016.

[21] P. Finkel, M. Staruch, A. Amin, M. Ahart, and S. E. Lofland, “Simultaneous Stress and Field Control of Sustainable Switching of Ferroelectric Phases.,” Sci. Rep., vol. 5, p. 13770, 2015, doi: 10.1038/srep13770.

[22] B. W. L. Puskas and T. Piazza, “Designer Waveforms: Ultrasonic Technologies to Improve Cleaning and Eliminate Damage,” no. August, pp. 1–9, 2001.

[23] M. R. Sadiq, “Enhanced Biopsy and Regional Anaesthesia through Ultrasound Actuation of a Standard Needle By Muhammad Rohaan Sadiq,” no. February, 2013.

[24] K. F. Graff, Power ultrasonic transducers: Principles and design. Elsevier Ltd., 2015.

[25] M. Lucas and A. Mathieson, Ultrasonic cutting for surgical applications. Elsevier Ltd., 2015.

[26] M. E. Schafer, Ultrasonic surgical devices and procedures. Elsevier Ltd., 2015.

[27] Stryker, “SONOPET,” 2020. https://neurosurgical.stryker.com/products/sonopet-ultrasonic-aspirator/ (accessed Apr. 28, 2020).

[28] Soring, “Ultrasonic assisted bone intrument.” https://www.soering.de/en/products/bone-instrument/ (accessed Apr. 28, 2020).

[29] IDOM, “Surgical Ultrasonic Bone-Cutting Device.” https://www.idom.com/project/surgical-ultrasonic-bone-cutting-device/ (accessed Apr. 28, 2020).

[30] A. MacBeath, “Ultrasonic Bone Cutting,” University of Glasgow, 2006.

[31] S. Cochran, “Piezoelectricity and basic configurations for piezoelectric ultrasonic transducers,” in Ultrasonic Transducers: Materials and Design for Sensors, Actuators and Medical Applications, Woodhead Publishing Limited, 2012, pp. 3–35.

[32] T. Consulting, “Ultrasonic Vessel Sealing and Dissection Devices,” 2017. https://www.youtube.com/watch?v=dR0H9no9yME (accessed May 05, 2020).

[33] Ethicon, “Ethicon Product Catalog by Category.” https://www.ethicon.com/na/system/files?file=2020-03/035213-191202-Ethicon-Product-Catalog-Submission-File-v3.pdf (accessed Apr. 24, 2020).

[34] S. D. McCarus and L. K. S. Parnell, “The Origin and Evolution of the HARMONIC® Scalpel,” Gynecol. Surg. Technol. Int., vol. 35.

[35] B. J. O’Daly, E. Morris, G. P. Gavin, J. M. O’Byrne, and G. B. McGuinness, “High-power low-frequency ultrasound: A review of tissue dissection and ablation in medicine and surgery,” J. Mater. Process. Technol., vol. 200, no. 1–3, pp. 38–58, 2008, doi: 10.1016/j.jmatprotec.2007.11.041.

[36] J. Li, H. Liu, J. Li, Y. Yang, and S. Wang, “Piezoelectric transducer design for an ultrasonic scalpel with enhanced dexterity for minimally invasive surgical robots,” Proc. Inst. Mech. Eng. Part C J. Mech. Eng. Sci., vol. 234, no. 7, pp. 1271–1285, 2020, doi: 10.1177/0954406219892750.

[37] S. Sherrit et al., “Novel horn designs for ultrasonic/ sonic cleaning, welding, soldering, cutting, and drilling,” Smart Struct. Mater. 2002 Smart Struct. Integr. Syst., vol. 4701, no. May, pp. 353–360, 2002, doi: 10.1117/12.474671.

[38] S. A. Askins, M. A. Us, and B. Dolgin, “Folded_horn_patent_US20040047485A1 (Done 1652020),” vol. 1, no. 19, 2004.

[39] A. Feeney and M. Lucas, “A Comparison of Two Configurations for a Dual-Resonance Cymbal Transducer,” IEEE Trans. Ultrason. Ferroelectr. Freq. Control, vol. 65, no. 3, pp. 489–496, 2018, doi: 10.1109/TUFFC.2018.2793310.

[40] A. Feeney, “Nitinol Cymbal Transducers for Tuneable Ultrasonic Devices,” 2014, [Online]. Available: http://theses.gla.ac.uk/%5Cnhttp://theses.gla.ac.uk/5805/.

[41] F. Bejarano, A. Feeney, and M. Lucas, “A cymbal transducer for power ultrasonics applications,” Sensors Actuators, A Phys., vol. 210, pp. 182–189, 2014, doi: 10.1016/j.sna.2014.02.024.

[42] R. Lockhart et al., “Silicon micromachined ultrasonic scalpel for the dissection and coagulation of tissue,” Biomed. Microdevices, vol. 17, no. 4, pp. 1–12, 2015, doi: 10.1007/s10544-015-9981-6.

[43] A. Lal and R. M. White, “Silicon microfabricated horns for power ultrasonics,” Int. Conf. Solid-State Sensors Actuators, Eurosensors IX, Proc., vol. 1, pp. 405–408, 1995, doi: 10.1109/sensor.1995.717221.

[44] T. Jiang, C. Xia, S. Cochran, and Z. Huang, “Improved performance of d31-mode needle-actuating transducer with PMN-PT piezocrystal,” IEEE Trans. Ultrason. Ferroelectr. Freq. Control, vol. 65, no. 8, pp. 1415–1422, 2018, doi: 10.1109/TUFFC.2018.2838566.

[45] N. Velotti et al., “Comparison between LigaSure and Harmonic in Laparoscopic Sleeve Gastrectomy : A Single-Center Experience on 422 Patients,” vol. 2019, 2019.

[46] H. Krentel, H. C. Verhoeven, L. A. Torres-de, and R. L. De Wilde, “Laparoscopic ultrasonic dissectors : technology update by a review of literature,” pp. 1–7, 2019.

[47] B. Person, Æ. D. A. Vivas, Æ. D. Ruiz, Æ. M. Talcott, J. E. Coad, and Æ. S. D. Wexner, “Comparison of four energy-based vascular sealing and cutting instruments : A porcine model,” pp. 534–538, 2008, doi: 10.1007/s00464-007-9619-8.

[48] K. J. Wikiel, T. N. Robinson, and E. L. Jones, “Energy in robotic surgery,” no. November 2019, pp. 1–9, 2020, doi: 10.21037/ales.2020.03.06.

[49] S. C. Yang, J. Ahn, J. H. Kim, J. W. Yi, M. H. Hur, and K. Lee, “Comparison of the vessel sealer Extend ® with harmonic ACE ® in robotic bilateral axillary-breast approach thyroid surgery,” vol. 9, no. 2, pp. 164–171, 2020, doi: 10.21037/gs.2020.01.18.

[50] X. Yu, J. Zhou, H. Liang, Z. Jiang, and L. Wu, “Progress in Materials Science Mechanical metamaterials associated with stiffness , rigidity and compressibility : A brief review,” Prog. Mater. Sci., vol. 94, pp. 114–173, 2018, doi: 10.1016/j.pmatsci.2017.12.003.

Claims:

1. An ultrasonic transducer for surgical applications, the ultrasonic transducer being a Langevin transducer comprising:

a back mass;

a front mass;

an ultrasonic actuator arrangement held between the back mass and the front mass;

an ultrasonic horn arrangement forward of the front mass,

wherein vibrations generated by the ultrasonic actuator arrangement are conducted into the front mass and into the ultrasonic horn arrangement along a vibrational energy transfer path and are amplitude amplified by the ultrasonic horn arrangement,

wherein one or more of the back mass, front mass and ultrasonic horn arrangement includes a plurality of openings intersecting the vibrational energy transfer path and configured to provide an increased mechanical compliance in a direction along the vibrational energy transfer path, the plurality of openings being provided through a wall of an annular portion of one or more of the back mass, front mass and/or ultrasonic horn arrangement, and arranged based on a square lattice, rectangular lattice, triangular lattice or hexagonal lattice.

2. An ultrasonic transducer according to claim 1 wherein the transducer is a bolted Langevin transducer.

3. An ultrasonic transducer according to any one of claims 1 to 2 wherein each opening has a substantially uniform cross section along its depth.

4. An ultrasonic transducer according to any one of claims 1 to 3 wherein the openings each have the same size.

5. An ultrasonic transducer according to any one of claims 1 to 4 wherein there are three or more openings.

6. An ultrasonic transducer according to any one of claims 1 to 5 wherein the length of the transducer, measured from the proximal end of the back mass to the distal end of the horn, along the vibrational energy transfer path, is not more than 40mm.

7. An ultrasonic transducer according to claim 6 wherein the maximum diameter of the transducer, measured in a direction perpendicular to the length, is not more than 15mm.

8. A surgical tool comprising an ultrasonic transducer according to any one of claims 1 to 7.

9. A method of operation of an ultrasonic transducer, the ultrasonic transducer being a Langevin transducer comprising:

a back mass;

09 08 24

a front mass;

an ultrasonic actuator arrangement held between the back mass and the front mass;

an ultrasonic horn arrangement forward of the front mass,

the method including applying an electrical signal to the ultrasonic actuator arrangement to generate vibrations to be conducted into the front mass and into the ultrasonic horn arrangement along a vibrational energy transfer path and amplitude amplified by the ultrasonic horn arrangement,

wherein one or more of the back mass, the front mass and the ultrasonic horn arrangement includes a plurality of openings intersecting the vibrational energy transfer path providing an increased mechanical compliance in a direction along the vibrational energy transfer path, the plurality of openings being provided through a wall of an annular portion of one or more of the back mass, the front mass and/or the ultrasonic horn arrangement, and arranged based on a square lattice, rectangular lattice, triangular lattice or hexagonal lattice.

10. A method according to claim 9 wherein the ultrasonic transducer is operated at a power in the range 10-1000 Wcm^{-2}.

09 08 24